

---

Doctoral Dissertations

Student Theses and Dissertations


---

Summer 2016

## Fully differential study of projectile coherence effects in ionization of molecular hydrogen and atomic helium

Thusitha Priyantha Arthanayaka

Follow this and additional works at: [https://scholarsmine.mst.edu/doctoral\\_dissertations](https://scholarsmine.mst.edu/doctoral_dissertations)

 Part of the [Atomic, Molecular and Optical Physics Commons](#)

Department: Physics

---

### Recommended Citation

Arthanayaka, Thusitha Priyantha, "Fully differential study of projectile coherence effects in ionization of molecular hydrogen and atomic helium" (2016). *Doctoral Dissertations*. 2506.  
[https://scholarsmine.mst.edu/doctoral\\_dissertations/2506](https://scholarsmine.mst.edu/doctoral_dissertations/2506)

This thesis is brought to you by Scholars' Mine, a service of the Missouri S&T Library and Learning Resources. This work is protected by U. S. Copyright Law. Unauthorized use including reproduction for redistribution requires the permission of the copyright holder. For more information, please contact [scholarsmine@mst.edu](mailto:scholarsmine@mst.edu).

FULLY DIFFERENTIAL STUDY OF PROJECTILE COHERENCE EFFECTS IN  
IONIZATION OF MOLECULAR HYDROGEN AND ATOMIC HELIUM

by

W K ARTHANAYAKA MUDIYANSELAGE THUSITHA PRIYANTHA

ARTHANAYAKA

A DISSERTATION

Presented to the Faculty of the Graduate School of the  
MISSOURI UNIVERSITY OF SCIENCE AND TECHNOLOGY

In Partial Fulfillment of the Requirements for the Degree

DOCTOR OF PHILOSOPHY

in

PHYSICS

2016

Approved

Michael Schulz, Advisor  
Don H. Madison  
Jerry L. Peacher  
Daniel Fischer  
V.A. Samaranayake

© 2016

W K Arthanaayaka Mudiyansele Thusitha Priyantha Arthanayaka

All Rights Reserved

## **PUBLICATION DISSERTATION OPTION**

This dissertation consists of the following four articles, formatted in the style used by the JOURNAL OF PHYSICS B.

Pages 14-27 intended for submission to the JOURNAL OF PHYSICS B ON ATOMIC MOLECULAR AND OPTICAL PHYSICS.

Pages 28-44 intended for submission to the JOURNAL OF PHYSICS B ON ATOMIC MOLECULAR AND OPTICAL PHYSICS.

Pages 45-60 intended for submission to the JOURNAL OF PHYSICS B ON ATOMIC MOLECULAR AND OPTICAL PHYSICS.

Pages 61-77 intended for submission to the JOURNAL OF PHYSICS B ON ATOMIC MOLECULAR AND OPTICAL PHYSICS.

## ABSTRACT

It has been well established, that projectile coherent properties are important for the study of atomic fragmentation processes. Recent studies of ionization of molecular hydrogen had demonstrated that measured double differential cross sections (DDCS) are very sensitive to the coherent length of the projectile. These measurements have been performed with varied coherence length of the projectiles by controlling the geometry of the collimating slits, which are placed before the target. Later, fully differential cross sections (FDCS) for a coherent and an incoherent projectile beam has been study for the same collision system and the results confirmed the important role of intrinsic projectile coherence properties. In the study, a new insight into the interference term as a function of the phase angle was obtained. By analyzing the FDCS as a function of the momentum transfer and of the recoil-ion momentum, single-center interference and two-center interference were identified and separated from each other. Single-center interference could be studied selectively and in detail by measuring FDCS for ionization of helium, because two-center interference is obviously absent. *Ab initio* calculations were able to well reproduce the data, in which the projectiles are described by a wave packet of varying width. This comparison shows that single-center interference is due to a coherent superposition of a range of impact parameters leading to the same scattering angle.

## ACKNOWLEDGMENTS

First and foremost, I would like to express my sincere gratitude to my advisor Dr. Michael Schulz for the continuous support of my PhD study and related research, for his patience, motivation, and immense Knowledge. I would like to thank you for encouraging my research and for allowing me to grow as a research scientist. Besides my advisor, I would also like to show gratitude to my committee: Dr. Don Madison, Dr. Jerry Peacher, Dr. Daniel Fischer, and Dr. V. Samaranayake for their insightful comments and encouragement, but also for the hard questions which incited me to widen my research from various perspective. I would especially like to thank Dr. Ahmad Hasan for assisting me with KMAX data acquisition and data analysis application software and his patient with my knowledge gaps in the area.

I thank my fellow lab mates: Basu Lamichhane, Sachin Sharma, Sudip Gurung, Juan Remolina, Li shen, and Kisra Egodapitiya, for the stimulation discussions, for the sleepless nights we were working together, and for all the moments we have had in the last five years. Also, I thank my friends at Missouri S&T. In particular, I am grateful to Nilanka Gurusinghe and Sumudu Herath who opened home and heart to me when I first arrived in the city. Getting through my dissertation required more than academic support, I want to thank Pam Crabtree, Russ Summers, Ronald Woody, and Jan Gargus for all their help. Most importantly, none of this could have happened without my family. I would like to thank my family: my parents (late) and to my sister for supporting me throughout my academic career. Last but not the least, I would like to thank my wife, Kaushalya Amunugama, for her support, encouragement, quiet patience, and immense love.

## TABLE OF CONTENTS

	Page
PUBLICATION DISSERTATION OPTION .....	iii
ABSTRACT .....	iv
ACKNOWLEDGMENTS .....	v
LIST OF ILLUSTRATIONS .....	ix
 SECTION	
1. INTRODUCTION .....	1
 PAPER	
I. Separation of single-and two-center interference in ionization of H <sub>2</sub> by proton impact .....	14
Abstract .....	14
Introduction.....	14
Experiment.....	17
Results and Discussions.....	19
Conclusions.....	24
Acknowledgments .....	26
References.....	26
II. Influence of the post-collision interaction on interference effects in ionization of H <sub>2</sub> by proton impact .....	28
Abstract .....	28
Introduction.....	28
Experiment.....	31
Results and Discussions.....	32

Conclusions.....	41
Acknowledgements.....	42
References.....	42
III. Fully differential study of ionization in $p + H_2$ collisions near electron – projectile velocity matching.....	45
Abstract.....	45
Introduction.....	46
Experiment.....	48
Results and Discussions.....	49
Conclusions .....	58
Acknowledgements.....	58
References.....	58
IV. Fully differentials study of wave packet scattering in ionization of Helium by proton impact.....	61
Abstract.....	61
Introduction.....	61
Experiment.....	64
Results and Discussions.....	68
Conclusions.....	74
Acknowledgements.....	75
References.....	75



SECTION	
2. CONCLUSIONS.....	78
BIBLIOGRAPHY.....	83
VITA.....	86

## LIST OF ILLUSTRATIONS

		Page
Figure 1.1.	Ion impact single ionization process (a) before collision (b) after collision.....	3
Figure 1.2.	Three-dimensional angular distribution of ejected electron momenta for ionization of He by 100 MeV/a.m.u. $C^{6+}$ .....	5
Figure 1.3.	Double Differential cross sectional ratio for coherent and incoherent projectile beam as a function of projectile scattering angle in 75 keV proton impact on $H_2$ .....	10
Figure 1.4.	Fully differential cross section ratios between the coherent and incoherent projectile beam as a function of azimuthal angle for projectile energy loss of 30 eV and for fixed polar angles of (a) $35^\circ$ , and (b) $55^\circ$ .....	11
PAPER I		
Figure 1.	TDCS (top row) for $\theta_{el} = 35^\circ$ and $q$ (from left to right) = 0.71, 0.9, and 1.21 a.u. as a function of $\phi_{el}$ .....	20
Figure 2.	Illustration of the electron ejection geometry for the TDCS plotted in figure 1.....	22
Figure 3.	Ratios between TDCS for coherent and incoherent beams for electrons ejected into the scattering plane for $q$ (from panels a–d) = 0.71, 0.9, 1.21, and 1.86 a.u. and for electrons ejected into the perpendicular plane for $q = 0.71$ and 0.9 a.u. (panels e and f) as a function $\theta_{el}$ .....	24
Figure 4.	Ratios between TDCS for coherent and incoherent beams for $\theta_{el} = 35^\circ$ and $p_{recx} = 0.2$ a.u. as a function of $\phi_{el}$ . Curve: $I_s = 1 + \alpha \cos(qx \Delta b)$ and $qx$ from equation (1).....	25
PAPER II		
Figure 1.	Ratio $R$ between the double differential cross sections for coherent and incoherent projectile beams for a fixed energy loss of 57 eV as a function of scattering angle.....	34
Figure 2.	Longitudinal momentum spectrum for the ejected electrons (top panel) and the recoiling target ions (bottom panel).....	35

Figure 3.	Ratio between the cross sections with a condition on $p_{rz} = -1.0$ to $-0.1$ a.u. and the cross sections with a condition on $p_{rz} = -0.1$ to $1.0$ a.u. as a function of scattering angle for a fixed energy loss of $57$ eV and taken for the coherent projectile beam.....	36
Figure 4.	Same as figure 1, but with the additional condition $p_{rz} = -1.0$ to $-0.1$ a.u. (closed symbols) and $p_{rz} = -0.1$ to $1.0$ a.u. (open symbols). ..	38
Figure 5.	Ratio R between the double differential cross sections for coherent and incoherent projectile beams for a fixed energy loss of $30$ eV (open symbols) and of $57$ eV with the additional condition $p_{rz} = -0.1$ to $1.0$ a.u. as a function of scattering angle....	40
PAPER III		
Figure 1.	Fully differential cross sections for electrons with an energy of $41.6$ eV ejected into the scattering plane as a function of the polar electron emission angle. ....	54
Figure 2.	Fully differential cross sections for electrons with an energy of $41.6$ eV ejected along the surface of a cone with an opening angle of $35^\circ$ as a function of the azimuthal electron emission angle.. ....	55
PAPER IV		
Figure 1.	Ratios between double differential cross sections measured for coherent and incoherent projectile as a function of scattering angle (closed symbols, lower scale) and the x-component of the recoil-ion momentum (open symbols, upper scale)....	70
Figure 2.	Fully differential cross sections for fixed projectile energy loss ( $\epsilon = 30$ eV) and fixed x-component of the recoil-ion momentum ( $p_{recx} = 1.25$ a.u.) as a function of the azimuthal and polar electron emission angles. ....	72
Figure 3.	Ratios between FDCS for coherent and incoherent beams $p_{recx} = 0.2$ a.u. and $\theta_{el} = 25^\circ$ (panel a), $p_{recx} = 0.7$ a.u. and $\theta_{el} = 45^\circ$ (panel b), $p_{recx} = 0.7$ a.u. and $\theta_{el} = 65^\circ$ (panel c), and $p_{recx} = 1.25$ a.u. and $\theta_{el} = 65^\circ$ (panel d) as a function $\phi_{el}$ . ....	73

## SECTION

### 1. INTRODUCTION

In order to study natural phenomena on a fundamental level, two major questions need to be addressed. First the forces acting between particles need to be understood and in nature there are four fundamental forces, namely the gravitational, electromagnetic, weak, and strong forces. All of these fundamental forces are mediated by the exchange of gauge bosons. This means that the mediation of a force is essentially a two-body process, because the gauge boson can be emitted by only one particle and absorbed by one particle at a time. Out of these forces only the electromagnetic force is essentially fully understood. Second, we need to understand how systems with more than two particles develop in space and time under the influence of these pairwise forces. For such systems the Schrodinger equation cannot be solved analytically even if the underlying forces are precisely known and this fundamental problem is known as the few body problem (FBP). In order to address the FBP, sophisticated theoretical models have to be developed and detailed experimental data are required to test the accuracy of such models.

For 2 reasons, atomic collision experiments provide the best set up to test the accuracy of such models [1 - 3]. First the underlying force, the electro-magnetic force, is essentially completely understood. In contrast, the forces underlying nuclear systems, i.e. the weak and strong forces, are much less understood than the electro-magnetic force. In nuclear collision experiments, it is thus unclear whether the results test the theoretical description of the few-body dynamics or the theoretical description of the fundamental forces in the system. Second, in atomic collision experiments, systems with small particle

numbers can be investigated. For such small particle numbers kinematically complete experiments, where the complete kinematics of every particle in the system are determined, are feasible. In contrast, in solid state systems the particle number is of the order of the Avogadro number and kinematically complete experiments are not feasible. In such experiment only statistically averaged or collective quantities are obtained. As a result a potential lack of understanding of the few body dynamics could be hidden in the statistics over a huge particle number.

From a kinematically complete experiment fully differential cross sections (FDCS) can be extracted. Since the FDCS are not averaged over any kinematic parameters they offer the most sensitive test of theoretical models. In an atomic collision process several reactions could occur, like e.g. ionization, capture, and excitation. Single ionization is particularly well suited to study the FBP [4], because it has three unbound particles (the scattered projectile, the ejected electron and the recoil ion) in the final state of the collision, which is the smallest particle number pertinent to the FBP. Fig. 1.1 schematically illustrates the ion impact single ionization process. In the experiment a projectile ion  $B^+$  with initial momentum  $\mathbf{P}_0$ , collides with a target A. In order to perform a kinematically complete experiment at least two out of three momentum vectors of the collision fragments are to be measured directly. The momentum vector of the third collision fragment is then already determined by momentum conservation, because the initial momentum of the collision is known by the settings of the projectile accelerator.

FDCS measurements for ion impact only become feasible with the development of Cold Target Recoil Ion Momentum Spectroscopy (COLTRIMS) approximately 20 years ago [5-8]. COLTRIMS is a powerful technique to investigate the reaction dynamics with

atoms and molecules, which allows to measure all momentum components of the recoil ion with high resolution. There has been an increase of interest in COLTRIMS technique in a broad area of atomic physics ranging from charged-particle collisions, to simple photon interactions to intense laser fields.

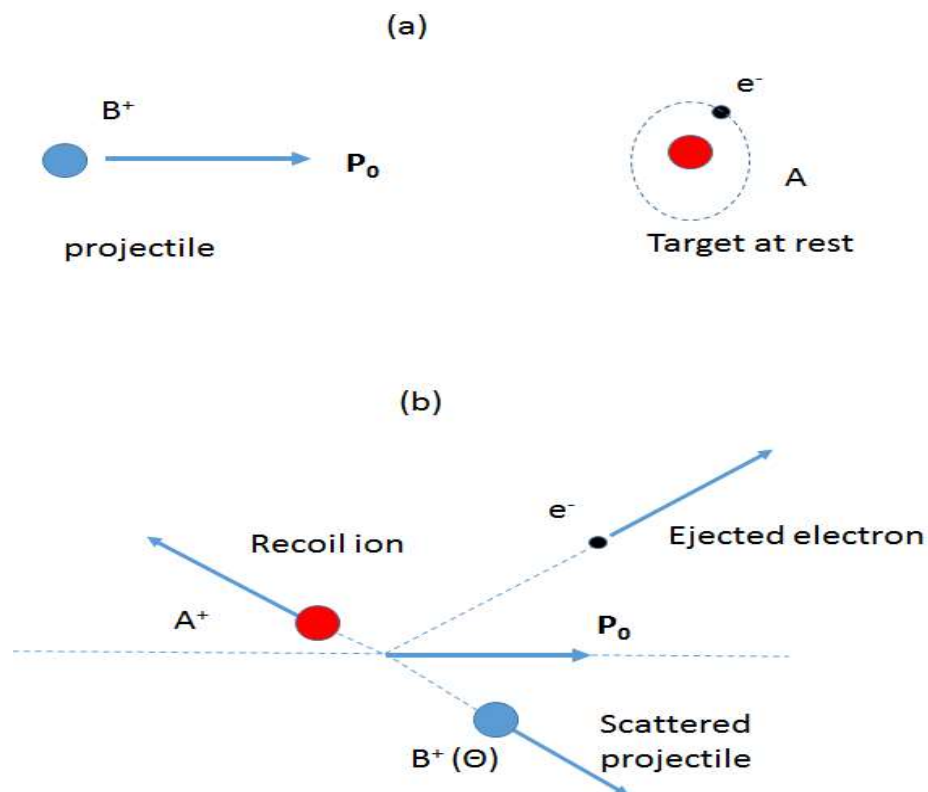


Figure 1.1. Ion impact single ionization process (a) before collision (b) after collision.

There are 3 possibilities to perform a kinematically complete experiment by measuring the momentum vectors of: (1) the projectile and the recoil ion, (2) the projectile and the electron and (3) the recoil ion and the electron. The undetected particle momentum is then obtained from momentum conservation. The direct measurement of the scattered projectile momentum in ion collision experiments is a tedious task especially for fast and

heavy ions, because the scattering angle of the projectile is in the range of mili-radians (mrad) or even much smaller. Furthermore the typical energy loss of such a scattered projectile is very small compared to its initial energy. The unique projectile momentum spectrometer at Missouri S&T allows the direct momentum analysis of the projectile ion up to energies of 200 keV [9, 10]. After a COLTRIMS apparatus has been added to the system [5-8], the projectiles and recoil ions can be detected and momentum is analyzed in a coincidence setup. For heavy and fast ions, the direct projectile-recoil ion measurement is impossible and there FDCS are studied by measuring the recoil ion and the ejected electron momentum in coincidence.

In atomic collision experiments the perturbation parameter ( $\eta$ ), i.e. the projectile charge to speed ratio, is an important parameter characterizing the nature of the collision process. Perturbative and non-perturbative theoretical models were able to reproduce the experimental data for system of small  $\eta$  in the scattering plane, which is spanned by the initial ( $\mathbf{P}_0$ ) and final ( $\mathbf{P}_f$ ) projectile momentum vectors. Even the relatively simple first born approximations (FBA) was able to reproduce the experimental data for electron impact for this kinematic region [11-13]. It was therefore believed, that the collision dynamics was basically understood for small  $\eta$  even for ion impact. Later, FDCS were measured for ion impact with electron ejected outside the scattering plane [14 - 16]. Surprisingly there even sophisticated higher-order theoretical models failed to reproduce the experimental data [17 - 19].

More specifically, Schulz et al [1] measured the FDCS for single ionization of He by 100 MeV/a.m.u  $C^{6+}$  ions. As an example a fully differential three dimensional angular distribution of the ejected electrons from this experiment is plotted in Fig. 1.2(a) for a

momentum transfer of  $q = 0.75$  a.u. and electron energy  $E_{el} = 6.5$  eV. The direction of the initial projectile beam is labeled as  $\mathbf{P}_0$  and the momentum transfer from the projectile to the target ( $\mathbf{P}_0 - \mathbf{P}_f$ ) is given by  $\mathbf{q}$ . In the data a pronounced peak structure approximately in the direction of  $\mathbf{q}$  is observed, which is known as the binary peak in the literature. This structure occurs due to a binary interaction between the projectile and the ejected electron. Furthermore, a smaller peak structure in the opposite direction of  $\mathbf{q}$  is known as recoil peak. This structure is due to an interaction between the projectile and the electron followed by

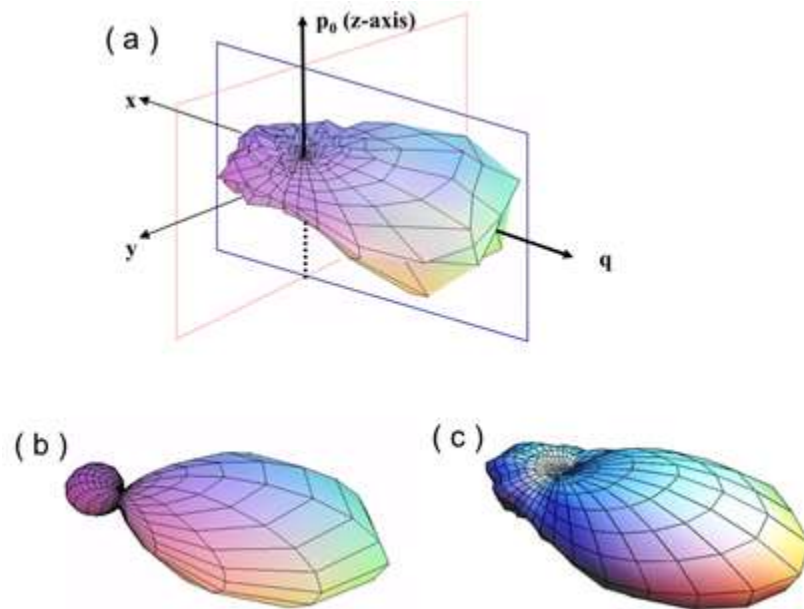


Figure 1.2. Three-dimensional angular distribution of ejected electron momenta for ionization of He by 100 MeV/a.m.u.  $C^{6+}$ . (a) Experiment (b) 3DW calculations (c) FBA convoluted with classical elastic scattering.

back-scattering from the target nucleus. Significant and qualitative discrepancies were found between the data and various theoretical calculations. For example, Fig. 1.2(b) shows a state of the art calculation, based on the three-body distorted wave (3DW) approach by Madison et al [20]. 3DW is a fully quantum mechanical perturbative model,



which considers higher-order contributions to the cross section in the final-state wave function.

The data are qualitatively and quantitatively well reproduced in the scattering plane (blue color plane) in Fig. 1.2. However, outside the scattering plane agreement is much worse. The 3DW calculation results in a pronounced two lobe structure separated by a sharp minimum at the origin. In contrast, in the experimental data this minimum is completely filled up. Some theoretical papers argued [21, 22] that, such effects are due to the experimental resolution. However a thorough analysis of the experimental resolution showed that it cannot explain the observed features alone [23, 24]. The suggested target temperature in the theoretical papers was over estimated by an order of magnitude compared to the actually realized temperature ( $\sim 1-2$  K).

Such discrepancies are common to all fully quantum mechanical models [18, 20, 25, 26] which raised the question whether all fully quantum mechanical approaches are sharing some fundamental problem. Indeed all of these models assumed a completely delocalized projectile (coherent projectile). For example, in the Born series the projectile is described in terms of a plane wave. However, such a massive and fast projectile ion is well localized due to its tiny de Broglie wave length and thus is better described in terms of wave packets with a narrow width, or in other words it has to be treated incoherently.

Fig. 1.2(c) shows a three dimensional angular distribution of the ejected electron for the same collision system. Here a FBA calculation is convoluted with classical elastic scattering between the heavy particles, which accounts for the interaction between the target nucleus and the projectile. In such a calculation the projectile is partly treated as a localized particle as far as interaction with the target nucleus is concerned. Surprisingly,

this supposedly less sophisticated semi-classical calculation qualitatively yield much improved agreement with experimental data and reproduces the filling of the minimum between the binary and recoil lobes [23, 24].

Egodapitiya et al [27] have discussed one possibility to test the effect of the coherence properties on atomic scattering cross sections by performing an experiment on single ionization of molecular  $H_2$ . It is well established that indistinguishable diffraction of the projectile from the two atomic centers of  $H_2$  can lead to interference structures, which is observable in the scattering angle dependence of the cross sections [28-31]. However one important requirement to observe interference structure is that the width of the projectile wave packet, or the transverse coherence length, must be larger than the effective size of the molecule [32]. Experimentally the width of the projectile wave packet (transverse coherence length  $\Delta r$ ) can be controlled by placing a collimating slit at a variable distance before the target. In analogy to classical optics,

$$\Delta r = \frac{\lambda L}{2a} \quad (1)$$

Where  $\Delta r$  is the transverse coherence length,  $\lambda$  is the de-Broglie wavelength of the projectile beam,  $L$  is the distance between the target and the collimating slits and  $a$  is the width of the collimating slit. If  $\Delta r$  is larger than the atomic separation  $d$  of the molecule, the projectile beam is coherent and an interference pattern should be observed, otherwise it is incoherent and no interference structure is observed.

Egodapitiya et al [27] measured double differential cross sections (DDCS), which is differential in the energy loss and in the solid angle of the projectile. The projectile

coherence length was varied by varying the slit distance to the target, yielding coherence lengths of 3.3 a.u. and less than 1 a.u., respectively. Since the separation of the two atomic centers  $d$  of  $H_2$  is 1.4 a.u., this means that a coherent beam is generated with a large slit distance and an incoherent beam with a small slit distance. An interference structure was found for the coherent beam, which was absent for the incoherent beam. That experiment thus qualitatively demonstrated the importance of the projectile coherence properties, a factor that was largely overlooked for decades of scattering theory.

In analogy to classical optics, the ratio  $R$  between the cross section (CS) for a coherent and an incoherent beam represents the interference term ( $IT$ ),

$$R = \frac{(CS)_{coherent}}{(CS)_{incoherent}} = IT \quad (2)$$

Theory predicts that the interference term for molecular two-center interference for fixed molecular orientation is given by

$$IT = 1 + \cos(\mathbf{p}_{rec} \cdot \mathbf{d}) = 1 + \cos \delta \quad (3)$$

Here the phase angle  $\delta$  of the interference term is given by the dot product of recoil ion momentum vector  $\mathbf{p}_{rec}$  and the inter-nuclear separation vector  $\mathbf{d}$  of the molecule. Since the molecular orientation is not measured in the experiment  $IT$  has to be averaged over all molecular orientations, which yields

$$IT = 1 + \frac{\sin(p_{rec}d)}{(p_{rec}d)} \quad (4)$$

Egodapitiya et al observed a pronounced structure in the double differential cross sectional ratio for coherent and incoherent projectile beam as a function of projectile scattering angle as shown in the Fig. 1.3 [27]. While this observation represents a strong indication that the projectile coherence properties play an important role in  $p + H_2$  collisions, it does not provide evidence those discrepancies in the  $C^{6+} + He$  experiment are due coherence effects [1]. Recently, an analogous experiment was performed by Wang et al [33] using  $p + He$  collision system. They have kept the  $\eta$  value equal to the  $C^{6+}$  experiment and a coherence length of about 5 a.u. was realized in the experiment. There, a more pronounced minimum was observed at the origin of the electron momentum distribution. Furthermore a recent experiment by Gassert et al [34] for  $p + He$  collisions at slightly larger  $\eta$  and  $\Delta r \approx 1-2$  a. u. also resulted in a pronounced minimum. These results seem to support the interpretation that the discrepancies between experiment and theory are indeed due to the projectile coherence properties.

More recently, Sharma et al [35] performed an experiment to study coherence and interference effects in more detail and more systematically by measuring and analyzing fully differential cross section (FDCS) at intermediate projectile energies. They have performed a kinematically complete coincidence experiment for ionization of  $H_2$  by 75 keV proton impact with varied coherence lengths for the projectile and for an energy loss  $\epsilon$  of 30 eV.

The FDCS were analyzed for fixed energy loss, transverse recoil ion momentum and polar electron ejection angle and plotted as a function of the azimuthal electron ejection angle ( $\phi_{e1}$ ). From the conservation law of momentum it is found that in this representation of the FDCS each  $\phi_e$  unambiguously corresponds to a well-defined momentum transfer. In

Fig. 1.4  $R$  (i.e. the interference term) is plotted as a function of  $\phi_{el}$  for  $\varepsilon = 30$  eV,  $p_{recx} = +0.2$  a.u. and  $\theta_{el} = 35^\circ$  (a) and  $\theta_{el} = 55^\circ$  (b). The structures in Fig. 1.4 shows that the cross sections depend on the coherence properties of the projectiles. Furthermore, these structures reflect an interference for which the phase angle depends on  $q$ . This was a surprising observation because the phase angle in molecular 2-center interference was expected to depend on the recoil ion momentum (which is fixed in Fig. 1.4) and not on  $q$ . Sharma et al considered two possibilities to explain this observation. First, the phase angle in molecular two-center interference may not be primarily determined by  $p_{rec}$ , but rather by  $q_x$ . Second, the dominant contribution to the interference may be due to some type other than two-center molecular interference.

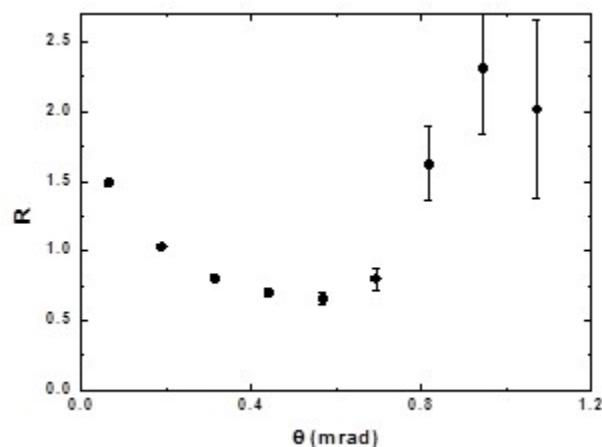


Figure 1.3. Double Differential cross sectional ratio for coherent and incoherent projectile beam as a function of projectile scattering angle in 75 keV proton impact on  $H_2$ .

More specifically, they considered the possibility of first- and higher-order ionization amplitudes interfering with each other, to which they referred as single-center

interference. From geometry the interference term for this type of interference can be shown to be given by

$$IT = 1 + \alpha \cos(q_x \Delta b) \quad (5)$$

where  $\Delta b$  is the impact parameter separation between the interfering amplitudes and  $\alpha$  accounts for damping of the interference structure due to incomplete coherence even at the largest slit distance and experimental resolution. The measured  $R$  can be well reproduced

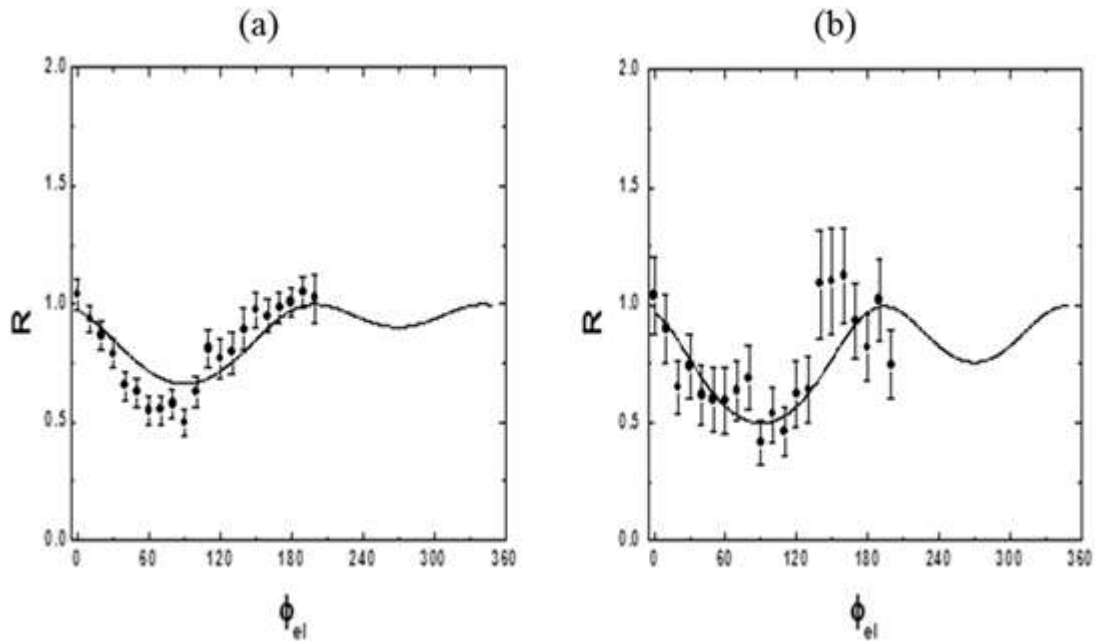


Figure 1.4. Fully differential cross section ratios between the coherent and incoherent projectile beam as a function of azimuthal angle for projectile energy loss of 30 eV and for fixed polar angles of (a) 35°, and (b) 55°. The x-component of the recoil-ion momentum is fixed at +0.2 a.u. The solid lines were obtained from  $1 + \alpha \cos(q_x \Delta b)$  for  $\Delta b = 2$  a.u. and  $\alpha = 0.5$ .

by this expression (solid curve in Fig. 1.4) for  $\Delta b = 2$  a.u. and  $\alpha = 0.5$ . In contrast, only a very weak dependence of the phase angle on  $p_{\text{rec}}$  was observed. These observations suggest that single center interference may be more important than two-center interference.

The previous work of Egodapitiya [27] et al and Sharma et al [35] demonstrated the importance of coherence properties on measured scattering cross sections. Both of these studies also led to new questions, which are still awaiting answers. First of all, the question whether the phase-angle dependence on  $q$  of the interference in the FDCS of Sharma et al is due to the single-center interference or due to other interference, is not settled yet. Furthermore, the nature of single-center interference needs to be investigated further. For example, another possibility is that single-center interference can also be regarded as interference between different impact parameters ( $b$ ) leading to same scattering angle ( $\Theta$ ). Even in a first order treatment a broad spectrum of  $b$  contributes to each  $\Theta$ . Therefore, it is not clear that higher-order contributions are needed to explain the single center interference. If they are needed one question is how important are such contributions. In this thesis a series of experiments was performed to address these questions in more detail.

In this dissertation, measured FDCS for single ionization of  $\text{H}_2$  by 75 keV proton impact at  $\epsilon = 57$  eV are presented. Earlier Alexander et al [36] found that interference is suppressed at this  $\epsilon$ . The motivation of this experiment was to investigate what leads to this suppression and whether this is related to the relative importance of single-center interference versus two-center interference. In the final part of this dissertation, FDCS measurements were performed for single ionization of He by 75 keV proton impact at  $\epsilon = 30$  eV. Here, obviously two-center interference is not present, which allows to study single-

center interference unambiguously without being obscured by other contributions. Comparison with new theoretical work enabled us to obtain a better understanding of single-center interference.



## PAPER

### I. Separation of single-and two-center interference in ionization of H<sub>2</sub> by proton impact

T. P. Arthanayaka<sup>1</sup>, S. Sharma<sup>1</sup>, B. R. Lamichhane<sup>1</sup>, A. Hasan<sup>1,2</sup>, J. Remolina<sup>1</sup>, S.

Gurung<sup>1</sup> and M. Schulz<sup>1</sup>

<sup>1</sup> Department of Physics and LAMOR, Missouri University of Science and Technology,  
Rolla, MO 65409, USA.

<sup>2</sup> Department of Physics, UAE University, PO Box 15551, Al Ain, Abu Dhabi, UAE

#### Abstract

We present a triple differential experimental study of ionization of molecular hydrogen by proton impact. By comparing cross-sections obtained for coherent and incoherent projectile beams we were able to extract contributions from interference. Two types of distinctly different interferences could be identified. We demonstrate that both types can be separated in the same data set by analyzing triple differential cross-sections for fixed momentum transfer and for fixed recoil-ion momentum.

#### Introduction

Interference and coherence effects in collisions of charged particles with molecular hydrogen have attracted a lot of interest in recent years [e.g. 1–11]. Two-center interference arises from indistinguishable electron ejection from or projectile diffraction off the two atomic centers in the molecule. However, the associated interference pattern can be quite difficult to observe. Several experiments attempted to observe it in the electron energy

spectra for fixed ejection angle [e.g. 1, 2]. But since no further kinematic information, like e.g. the molecular orientation or the momentum of the recoiling  $\text{H}_2^+$  ion, was extracted from these experiments the phase angle in the interference term was effectively averaged over these quantities so that the interference structure was rather weak. Alexander et al [6] measured double differential ionization cross-sections for fixed projectile energy loss as a function of the scattering angle. There, the interference pattern is superimposed on the steeply decreasing cross-sections with increasing scattering angle, which also makes it difficult to observe a pronounced structure.

In analogy to classical optics the cross-section can be expressed as a product between the cross-sections one would get if interference was not present, to which we refer as the incoherent cross-section, and the interference term. In an attempt to overcome the problems mentioned in the previous paragraph it is therefore common to analyze the interference term as the ratio between the measured and the incoherent cross-section [1–4, 6]. The obvious difficulty with this approach is that the incoherent cross-section is usually experimentally not easily accessible. It was therefore approximated as twice the theoretical [1, 6] or experimental [2] cross-section for atomic hydrogen or as the experimental cross-section for helium [3, 4]. The uncertainties associated with these approximations complicate the interpretation of the data. Furthermore, even in this ratio the interference pattern is in most cases not very pronounced. Consequently, the insight into the nature of the interference present in the data that can be gained from such studies is somewhat limited.

A few years ago, in an attempt to resolve puzzling discrepancies between theory and experiment on fully differential cross-sections for ionization of helium by 100 MeV

amu<sup>-1</sup> C<sup>6+</sup> impact [12], we demonstrated that interference structures observed for a coherent projectile beam vanish if an incoherent beam is prepared by altering the geometry of a collimating slit placed before the target region [8]. As in classical optics the transverse coherence length is given by  $\Delta r = \lambda L/2a$ , where  $\lambda$  is the de Broglie wavelength of the projectile beam and  $L$  and  $a$  are the distance of the collimating slit to the target and its width, respectively [13]. If  $\Delta r$  is larger than the dimension of the diffracting object the beam is coherent, and interference structures can be observed, but it is incoherent otherwise and interference structures vanish. Appropriately adjusting the geometry of the collimating slit thus offers the possibility of directly measuring incoherent cross-sections. Similar projectile coherence effects were also reported for neutral atoms scattered from a periodic potential generated by laser fields [13] and more recently for neutron reflection from gratings [14]. Furthermore, the authors of the latter work concluded that wave packet coherence effects (referring to single particles) should be sharply separated from coherence effects originating from an ensemble of particles emitted incoherently from an extended source. This conclusion was further supported by an accompanying theoretical analysis [15].

In a recent study of low-energy electron ejection ( $E_{el} = 14.6$  eV) in 75 keV p+H<sub>2</sub> collisions we used this sensitivity of the cross-sections to the projectile coherence properties to analyze interference effects in more detail. Directly measuring the interference term as the ratio between the coherent and incoherent cross-sections enabled us to conclude that the phase angle is primarily dependent on the momentum transfer [10, 11]. For molecular two-center interference, in contrast, theory predicted that the phase angle should depend on the momentum of the recoiling H<sub>2</sub><sup>+</sup> ion [e.g. 16]. We offered two

alternative explanations for this observation: either, the assumption of theory that the phase angle depends on the recoil-ion momentum is incorrect or the structures in the data of [10, 11] predominantly reflect interference between first- and higher-order transition amplitudes (involving e.g. the projectile—target nucleus interaction). We refer to this as single-center interference because it does not require multiple scattering centers in the target. The impact parameter dependence of both amplitudes is usually not the same, even for a fixed scattering angle. Rather, higher-order mechanisms tend to favor smaller impact parameters than the first-order process. On the other hand, the impact parameter is not an observable, i.e. in an experiment one cannot distinguish which path led to a specific scattering angle. Single-center interference can therefore be viewed as interference between two (or more) impact parameters leading to the same scattering angle. In a simple, geometrical model which we reported in [10] the phase angle for this type of interference indeed depends on the momentum transfer, rather than on the recoil ion momentum. Furthermore, the data seemed to be consistent with such a momentum transfer dependent phase angle. However, the data were not sensitive enough to conclusively distinguish between single- and two-center interference.

## **Experiment**

In this communication we present the results of a kinematically complete experiment on ionization of  $H_2$  by 75 keV proton impact for an electron energy of 41.4 eV. In this case we find the phase angle to significantly depend on the recoil ion momentum as well. The comparison between the interference terms for the small and large electron energies reveals that both types of interference are present: single-center interference, with a momentum

transfer dependent phase angle, dominates at small energies while molecular two-center interference, with a recoil-ion momentum dependent phase angle, becomes increasingly important with increasing electron energy. We were able to separate both types of interference by analyzing triple differential cross-sections (TDCS) for fixed momentum transfers and for fixed recoil-ion momenta.

The experiment was performed at Missouri S&T. A 75 keV proton beam intersected with a very cold ( $T \cong 1\text{--}2\text{K}$ ) neutral  $\text{H}_2$  beam generated by a supersonic gas jet. The transverse coherence length of the projectiles was varied by placing a collimating slit of fixed width  $a = 0.15$  mm at two different distances ( $L_1 = 6.5$  cm,  $L_2 = 50$  cm) from the target. These slit geometries correspond to coherence lengths of  $\Delta r_1 = 0.4\text{--}1.0$  a.u. (for more details explaining this range see [11]) and  $\Delta r_2 = 3.3$  a.u., respectively, which makes the beam incoherent in the former and coherent in the latter case relative to the internuclear separation of the molecule of 1.4 a.u.. The projectiles which did not charge-exchange in the collision were selected by a switching magnet, decelerated by 70 keV and energy-analyzed by an electrostatic parallel-plate analyzer [17]. The beam component which suffered an energy loss of 57 eV, corresponding to an electron energy of 41.6 eV, was detected by a two-dimensional position sensitive channel plate detector. From the position information in the x-direction (defined by the orientation of the analyzer entrance and exit slits) the x-component of  $\mathbf{q} = \mathbf{p}_o - \mathbf{p}_f$  (where  $\mathbf{p}_o$  and  $\mathbf{p}_f$  are the initial and final projectile momenta) could be determined. Because of the very narrow width of the analyzer slits (75  $\mu\text{m}$ ) the y-component of  $\mathbf{q}$  was fixed at 0 (within the experimental resolution) for all detected projectiles. The z-component (pointing in the projectile beam direction) of  $\mathbf{q}$  is given by  $q_z = \varepsilon/v_p$ , where  $\varepsilon$  and  $v_p$  are the energy loss and the speed of the projectiles. The

resolution in the x-, y-, and z-components of  $\mathbf{q}$  was 0.35, 0.2, and 0.07 a.u. full width at half maximum (FWHM), respectively.

The  $\text{H}_2^+$  ions produced in the collisions were extracted by a weak electric field of  $8 \text{ V cm}^{-1}$  and then drifted in a field free region, twice as long as the extraction region, before hitting another two-dimensional position-sensitive channel-plate detector. From the position information the y- and z-components of the recoil-ion momentum could be determined. The two detectors were set in coincidence and the coincidence time is, apart from a constant offset, equal to the time of flight of the recoil ions from the collision region to the detector. From it, the x-component of the recoil-ion momentum can be determined. The momentum resolution in the x-, y-, and z-direction was 0.15, 0.5, and 0.15 a.u. FWHM, respectively. Finally, the electron momentum was deduced from momentum conservation by  $\mathbf{p}_{\text{el}} = \mathbf{q} - \mathbf{p}_{\text{rec}}$ .

## Results and Discussions

In spite of the large total ionization cross-section for this collision system data were taken over a time period of several months. This is due to a combination of the triple differential nature of the data and the very small solid angle on the projectile momentum-analyzer which is necessary in order to achieve sufficient energy ( $\Delta E/E \approx 3 \times 10^{-5}$ ) and angular resolution ( $\Delta \theta \approx 0.12 \text{ mrad}$ ).

In the top panels of figure 1 we show TDCS for fixed  $q$  of 0.71 a.u. (left), 0.9 a.u. (center), and 1.21 a.u. (right) and for fixed polar electron emission angle  $\theta_{\text{el}} = 35^\circ$  (measured relative to the initial projectile beam axis) as a function of the azimuthal electron ejection angle  $\varphi_{\text{el}}$ . The electron ejection geometry is illustrated in figure 2. Keeping  $\theta_{\text{el}}$

fixed means that only electrons are analyzed with momentum vectors lying on the surface of a cone with an opening angle  $2\theta_{el}$  centered on the  $z$ -axis.  $\phi_{el}$  is the angle between the projection of  $\mathbf{p}_{el}$  onto the  $xy$ -plane and the positive  $y$ -axis, where the positive  $x$ -axis is defined by the direction of the transverse component of  $\mathbf{q}$ . The data plotted as the closed

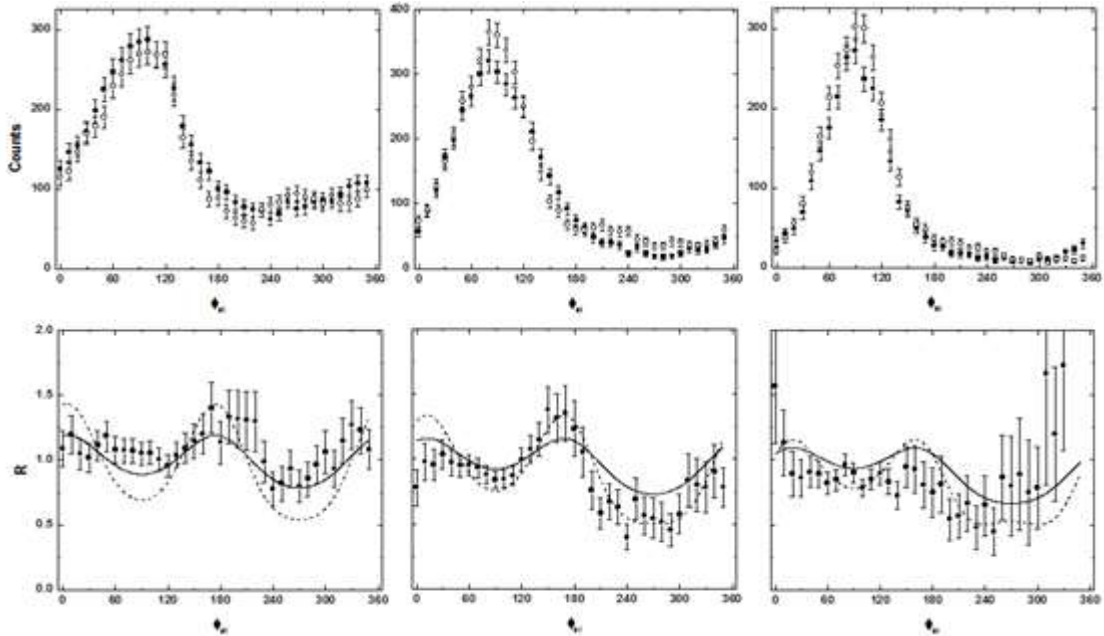


Figure 1. TDCS (top row) for  $\theta_{el} = 35^\circ$  and  $q$  (from left to right) = 0.71, 0.9, and 1.21 a.u. as a function of  $\phi_{el}$ . Closed symbols: coherent beam; open symbols: incoherent beam. Bottom row: ratios between TDCS for coherent and incoherent beams. Solid curves: It calculated with equation (2) for fixed (dashed curves) and random (solid curves) orientation.

(open) symbols were taken for the large (small) slit distance and in the following we refer to them as the coherent (incoherent) triple differential (in the projectile and electron solid angles and in the electron energy) cross-sections TDCS<sub>coh</sub> (TDCS<sub>inc</sub>). Relatively small, but significant and systematic differences between both data sets can be seen.

In analogy to classical optics the ratio  $R = \text{TDCS}_{\text{coh}} / \text{TDCS}_{\text{inc}}$  represents the interference term. It is plotted in the bottom panels of figure 1 for the same kinematics and in the same order as the actual TDCS. The structures in this ratio show that the phase angle in the interference term depends on the recoil-ion momentum. With  $\mathbf{q} = \mathbf{p}_{\text{rec}} + \mathbf{p}_{\text{el}}$  the recoil-ion momentum components are given by

$$\begin{aligned} p_{\text{rec}x} &= q_x - p_{\text{el}} \sin \varphi_{\text{el}} \sin \theta_{\text{el}} \\ p_{\text{rec}y} &= - p_{\text{el}} \cos \varphi_{\text{el}} \sin \theta_{\text{el}} \\ p_{\text{rec}z} &= \varepsilon / v_p - p_{\text{el}} \cos \theta_{\text{el}} \end{aligned} \quad (1)$$

Since  $q_x$ ,  $\varepsilon$  (and thereby  $p_{\text{el}}$ ) and  $\theta_{\text{el}}$  are fixed for each plot of figure 1,  $\mathbf{p}_{\text{rec}}$  is unambiguously determined by  $\varphi_{\text{el}}$  and the dependence of  $R$  on  $\varphi_{\text{el}}$  is thus equivalent to a dependence of  $R$  on  $\mathbf{p}_{\text{rec}}$ . In contrast, for  $\varepsilon = 30$  eV (corresponding to  $E_{\text{el}} = 14.6$  eV) we only observed a rather weak dependence of the phase angle on  $\mathbf{p}_{\text{rec}}$  [10, 11].

For two-center molecular interference it was assumed that the interference term is given by for fixed and random molecular orientations, respectively [e.g. 16], where  $\mathbf{D}$  is the internuclear separation vector.

$$\begin{aligned} I_{\text{f}} &= 1 + \cos (\mathbf{p}_{\text{rec}} \cdot \mathbf{D}) \quad \text{or} \\ I_{\text{r}} &= 1 + \sin (\mathbf{p}_{\text{rec}} \cdot \mathbf{D}) / (\mathbf{p}_{\text{rec}} \cdot \mathbf{D}) \end{aligned} \quad (2)$$

Note that due to the averaging over all molecular orientations, which are contained in the dot product  $\mathbf{p}_{\text{rec}} \cdot \mathbf{D}$ , the phase angle in the resulting interference term for random orientations is given by the magnitude product  $p_{\text{rec}} D$ . From the weak dependence of  $R$  on



$\mathbf{p}_{\text{rec}}$  for  $\varepsilon = 30$  eV, while at the same time we observed a strong dependence on  $q$ , we concluded that either the phase angle is determined by  $q$  instead of  $\mathbf{p}_{\text{rec}}$  or that the structure in  $R$  primarily reflects a different type of interference. More specifically, we discussed the possibility that interference between first- and higher-order transition amplitudes may lead to the structure and that the corresponding interference term would be determined by the transverse component of  $\mathbf{q}$ .

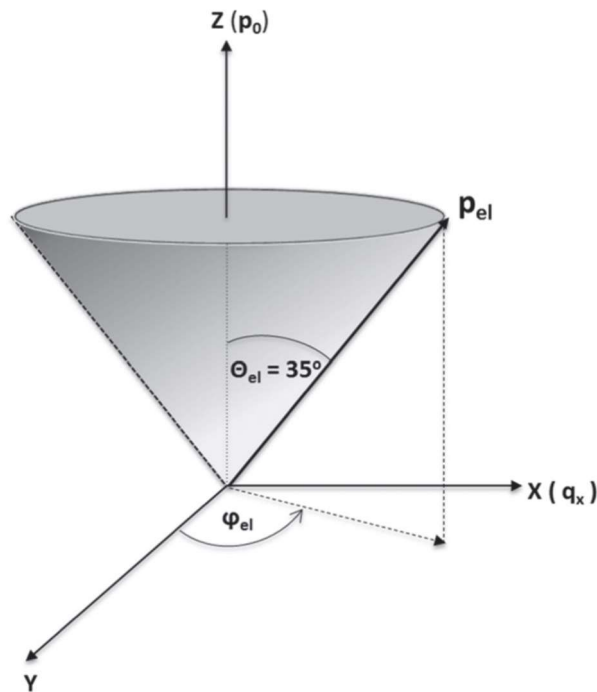


Figure 2. Illustration of the electron ejection geometry for the TDCS plotted in figure 1. The polar angle  $\theta_{\text{el}}$  is fixed at  $35^\circ$  so that for all electrons analyzed in figure 1 the momentum vectors lie on the surface of a cone with an opening angle of  $70^\circ$  centered on the  $z$ -axis.  $\varphi_{\text{el}}$  is the angle between the projection of the electron momentum onto the  $xy$ -plane and the positive  $y$ -axis.

The dependence of  $R$  on  $\mathbf{p}_{\text{rec}}$  in the present data shows that some type of interference with a  $\mathbf{p}_{\text{rec}}$ -dependent phase angle can be experimentally observed. It is certainly reasonable to interpret this structure as two-center molecular interference. In figure 1 we

therefore compare the data to the  $I_t$  calculated with equations (2) for the fixed (dashed curves) and random (solid curves) orientations. Here, we introduced a factor  $\alpha$  in front of the trigonometric functions to account for damping of the interference pattern due to incomplete coherence (in case of the large slit distance) and experimental resolution effects [10, 11].  $\alpha$  was adjusted to give the best overall fit (for all analyzed data sets) to the measured  $R$ . For the fixed (random) orientation we find values of  $\alpha = 0.5$  (0.7). Both curves are in rather good agreement with the data for all  $q$ . The error bars are not small enough to conclusively determine whether  $I_t$  for the fixed or the random orientation is in better agreement with the data. However, overall the measured  $R$  seem to slightly favor the random orientation, as one would expect. Nevertheless, a non-uniform distribution of the molecular orientation, as reported for electron impact [18], cannot be ruled out.

Using the same  $I_t$  calculated with the same values of  $\alpha$  we can also reproduce the coherent to incoherent cross-section ratios for other electron ejection geometries. In figure 3 panels (a) through (d) we show  $R$  for electrons ejected into the scattering plane and for momentum transfers fixed at 0.71 a.u., 0.9 a.u., 1.21 a.u., and 1.86 a.u. as a function of  $\theta_{el}$ . The scattering plane (or xz-plane) is spanned by  $\mathbf{p}_0$  and  $\mathbf{q}$ , i.e. for this plane  $\varphi_{el}$  is fixed at  $90^\circ$  for the range  $\theta_{el}=0-180^\circ$  and at  $270^\circ$  for the range  $\theta_{el}=180-360^\circ$ . Panels (e) and (f) of figure 3 show the ratios for electrons ejected into the plane perpendicular to the transverse component of  $\mathbf{q}$  (i.e. the yz-plane) for  $q = 0.71$  a.u. and 0.9 a.u. as a function of  $\theta_{el}$ . In all cases  $I_t$  calculated both for the fixed (dashed curves) and random molecular orientation (solid curves) are in good agreement with the measured  $R$ , where for the scattering (perpendicular) plane the data seem to slightly favor a fixed (random) orientation.

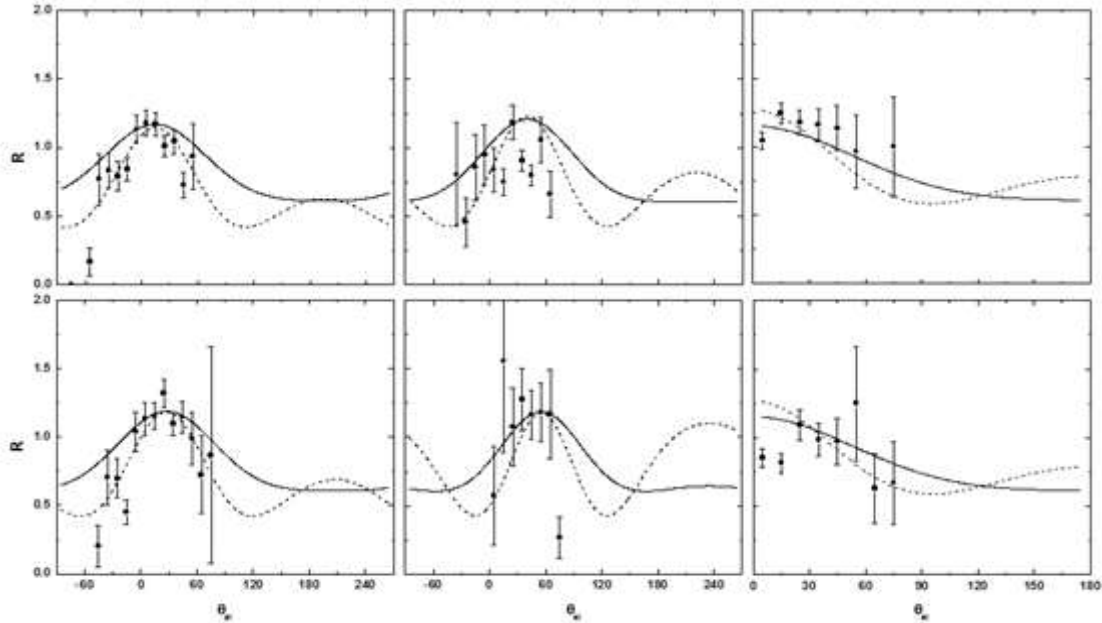


Figure 3. Ratios between TDCS for coherent and incoherent beams for electrons ejected into the scattering plane for  $q$  (from panels a–d) = 0.71, 0.9, 1.21, and 1.86 a.u. and for electrons ejected into the perpendicular plane for  $q$  = 0.71 and 0.9 a.u. (panels e and f) as a function  $\theta_{el}$ . Curves same as in figure 1.

## Conclusions

Based on the sensitivity of the structures observed in the measured  $R$  on  $\mathbf{p}_{rec}$  and based on the good agreement of  $I_t$  with  $R$ , we conclude that the TDCS are significantly affected by molecular two-center interference. This also implies that the phase angle in two-center interference is indeed determined by the recoil-ion momentum, as predicted by theory e.g. [16], and not by the momentum transfer, which we considered as one possible explanation for the  $q$ -dependent structures which we observed for  $\varepsilon = 30$  eV. This, in turn, means that the structures we observed for  $\varepsilon = 30$  eV are due to single-center interference between first- and higher-order amplitudes, which was the second possible explanation we considered for the  $q$ -dependence of the interference term [10, 11]. However, the  $\mathbf{p}_{rec}$ -dependence observed

in the present data for  $\varepsilon = 57$  eV does not necessarily mean that single-center interference does not play any role. Since the TDCS of figure 1 and 3 are plotted for fixed  $q$  its presence would only manifest itself in an overall factor in  $R$ , but it would not affect the shape of the  $\varphi_{el}$ -dependence of  $R$ .

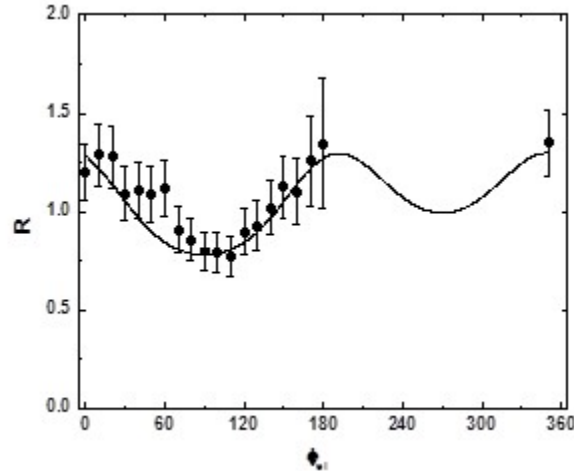


Figure 4. Ratios between TDCS for coherent and incoherent beams for  $\theta_{el} = 35^\circ$  and  $p_{reco} = 0.2$  a.u. as a function of  $\varphi_{el}$ . Curve:  $I_s = 1 + \alpha \cos(q_x \Delta b)$  and  $q_x$  from equation (1).

In order to analyze potential contributions from single-center interference, in figure 4 we show TDCS ratios in the same representation as in figure 1, except instead of  $q$  here  $p_{reco}$  is fixed at 0.2 a.u. In this case any dependence of  $R$  on  $\varphi_{el}$  is equivalent to a dependence on  $q_x$  signifying single-center interference. Indeed, a pronounced structure can be seen and the data look very similar to what we observed for  $\varepsilon = 30$  eV [11]. Furthermore, the measured  $R$  can be well reproduced by the same model interference term  $I_s = 1 + \alpha \cos(q_x \Delta b)$  (solid curve in figure 4) which yielded good agreement with the data for  $\varepsilon = 30$  eV. However, for  $\varepsilon = 57$  eV the damping factor is smaller ( $\alpha = 0.3$ ) than for the smaller energy

loss ( $\alpha = 0.5$ ) suggesting that single-center interference is less pronounced at larger energy losses.

In summary, from the structures found in R we conclude that both single- and two-center interference can be important in ionization of  $H_2$  and that these can be separated by analyzing TDCS for fixed  $q$  and for fixed recoil-ion momentum.

### Acknowledgments

Support of this work by the National Science Foundation (grant no. PHY-1401586) is gratefully acknowledged.

### References

- [1] Stolterfoht N et al 2001 Phys. Rev. Lett. 87 23201.
- [2] Misra D, Kadhane U, Singh Y P, Tribedi L C, Fainstein P D and Richard P 2004 Phys. Rev. Lett. 92 153201.
- [3] Milne-Brownlie D S, Foster M, Gao J, Lohmann B and Madison D H 2006 Phys. Rev. Lett. 96 233201.
- [4] Staicu Casagrande E M et al 2008 J. Phys. B: At. Mol. Opt. Phys. 41 025204.
- [5] Schmidt L P H, Schössler S, Afaneh F, Schöffler M, Stiebing K E, Schmidt-Böcking H and Dörner R 2008 Phys. Rev. Lett. 101 173202.
- [6] Alexander J S, Laforge A C, Hasan A, Machavariani Z S, Ciappina M F, Rivarola R D, Madison D H and Schulz M 2008 Phys. Rev. A 78 060701(R).
- [7] Misra D et al 2009 Phys. Rev. Lett. 102 153201.
- [8] Egodapitiya K N, Sharma S, Hasan A, Laforge A C, Madison D H, Moshhammer R and Schulz M 2011 Phys. Rev. Lett. 106 153202.
- [9] Sharma S, Hasan A, Egodapitiya K N, Arthanayaka T P and Schulz M 2012 Phys. Rev. A 86 022706.

- [10] Sharma S, Arthanayaka T P, Hasan A, Lamichhane B R, Remolina J, Smith A and Schulz M 2014 Phys. Rev. A 89 052703.
- [11] Sharma S, Arthanayaka T P, Hasan A, Lamichhane B R, Remolina J, Smith A and Schulz M 2014 Phys. Rev. A 90 052710.
- [12] Schulz M, Moshhammer R, Fischer D, Kollmus H, Madison D H, Jones S and Ullrich J 2003 Nature 422 48.
- [13] Keller C, Schmiedmayer J and Zeilinger A 2000 Opt. Commun. 179 129.
- [14] Majkrzak C F, Metting C, Maranville B B, Dura J A, Satija S, Udovic T and Berk N F 2014 Phys. Rev. A 89 033851.
- [15] Berk N F 2014 Phys. Rev. A 89 033852.
- [16] Corchs S E, Rivarola R D, McGuire J H and Wang Y D 1994 Phys. Scr. 50 469.
- [17] Gaus A D, Htwe W, Brand J A, Gay T J and Schulz M 1994 Rev. Sci. Instrum. 65 3739.
- [18] Senftleben A, Pflüger T, Ren X, Al-Hagan O, Najjari B, Madison D H, Dorn A and Ullrich J 2010 J. Phys. B: At. Mol. Opt. Phys. 43 081002.

## II. Influence of the post-collision interaction on interference effects in ionization of $H_2$ by proton impact

T.P. Arthanayaka<sup>1</sup>, S. Sharma<sup>1</sup>, B.R. Lamichhane<sup>1</sup>, A. Hasan<sup>1,2</sup>, J. Remolina<sup>1</sup>, S.

Gurung<sup>1</sup>, and M. Schulz<sup>1</sup>

<sup>1</sup>Dept. of Physics and LAMOR, Missouri University of Science & Technology, Rolla,  
MO 65409

<sup>2</sup>Dept. of Physics, UAE University, P.O. Box 15551, Al Ain, Abu Dhabi, UAE

### Abstract

We have performed a kinematically complete experiment on ionization of  $H_2$  by 75 keV proton impact leading to electrons with a speed equal to the projectile speed. By comparing cross sections measured with a coherent and an incoherent projectile beam we were able to perform a detailed analysis of interference effects. We found that the interference structure is significantly more damped than for smaller electron energies studied previously. This damping is further increased if kinematic conditions are selected which favor a strong role of the post-collisional interaction between the scattered projectile and the electron ejected to the continuum by a preceding primary interaction with the projectile.

### Introduction

The reaction dynamics of ionization of simple atoms by ion-impact has been studied extensively in kinematically complete experiments over the last decade [e.g. 1-5, for a recent review see 6]. The features in the three-dimensional electron ejection angle dependence of the resulting fully differential cross sections (FDCS) are in most cases remarkably simple. These data tend to be dominated by a pronounced peak structure

approximately in the direction of the momentum transfer  $\mathbf{q}$  (defined as the difference between the initial and scattered projectile momenta) known as the binary peak. For certain kinematic conditions a second less pronounced maximum, dubbed the recoil peak, is observed in the direction of  $-\mathbf{q}$ . The qualitative shape of this basic double lobe pattern is not even strongly altered when higher-order contributions are large. In spite of this simplicity the theoretical quantitative description of the reaction dynamics has proven to be quite challenging [e.g. 7-14].

One might suspect that the qualitative features in the FDCS for ionization of homonuclear molecules are essentially the same as for the corresponding atoms. However, one important difference between atomic and molecular targets is that for the latter the electron can be emitted from and the projectile scattered off either of the atomic centers in the molecule. The coherent sum of both contributions can lead to observable interference effects. Such structures were indeed reported in the ejected electron [e.g. 15, 16] and in double differential cross sections (DDCS) as a function of projectile scattering angle [17]. However, these experiments were not kinematically complete and as a result the spectra were partially averaged over the phase angle in the interference term thereby somewhat restricting the depth in the information extracted from the data.

More recently, we reported fully differential studies on contributions from interference to ionization in  $p + \text{H}_2$  collisions [18, 19]. One interesting result was that, apart from molecular two-center interference, single-center interference between first- and higher-order transition amplitudes, involving for example the interaction between the projectile and the target nuclei, also plays an important role and at small electron energies is, in fact, more important than two-center interference. The impact parameters



contributing to a specific scattering angle usually differ between first- and higher-order processes. Single-center interference can thus also be interpreted as an interference between different impact parameters leading to the same scattering angle.

These findings of references [18, 19] represent just one example of how fully differential data can provide more insight into the reaction dynamics than less differential data. However, there are many more questions relating to the reaction dynamics of ionization of molecular targets on which less differential studies so far did not provide answers. For example, in reference [17] we observed that the interference structures appeared to be much less pronounced for ejected electron energies corresponding to electron speeds  $v_e$  close to the projectile speed  $v_p$ . In that work we discussed a possible explanation which is based on two hypothetical assumptions: first, the apparent suppression of interference may be related to the post-collision interaction (PCI) between the outgoing projectile and the electron lifted to the continuum by a preceding primary interaction. It is well established that PCI effects maximize at  $v_e = v_p$  [20,21]. Second, the coherence required for observable interference may be lost (or at least reduced) for  $v_e \approx v_p$ . However, neither could we provide conclusive evidence for this explanation nor could we offer reasons as to why interference would be somehow linked to PCI (or lack thereof) or why coherence would be reduced in the presence of strong PCI.

The difficulties in performing a more conclusive analysis of the observations in reference [17] stem from two sources: first, the experiment was not kinematically complete, thereby compromising the level of detail in the data. Second, at the time it was not clear how the role of coherence could be experimentally tested. Since then both of these problems have been addressed: we have performed kinematically complete

experiments [18, 19, 22] and we demonstrated that the transverse projectile coherence length  $\Delta x$  can experimentally be varied by changing the geometry of a collimating slit in front of the target [23]. Indeed, for small  $\Delta x$  interference structures were found to be much less pronounced than at large  $\Delta x$ .

Performing kinematically complete experiments for different projectile coherence properties we could demonstrate that single- and two-center interference can be separated by analyzing the FDCS either for fixed momentum transfers or for fixed recoil-ion momenta [22]. However, a possible link between interference effects and PCI, as suggested in reference [17], was not addressed in that work. Here, we present the results of a kinematically complete experiment on ejection of target electrons with an energy corresponding to  $v_e = v_p$ . The data were analyzed under kinematic conditions either favoring or suppressing PCI. A comparison between multiple differential momentum spectra for these kinematic conditions suggests that single-center interference is significantly affected by PCI.

## Experiment

The details of the experiment were described previously [18]. In brief, a proton beam was generated by a hot cathode ion source and accelerated to an energy of 75 keV. The beam was collimated by an aperture with a diameter of 1.5 mm at the exit of the accelerator terminal and by a pair of vertical and horizontal slits, 150  $\mu\text{m}$  in width, placed at distance of  $L_1 = 50$  cm and  $L_2 = 6.5$  cm before the target region. The transverse coherence length was about  $\Delta x = 3.3$  a.u. for  $L_1$  and less than 1 a.u. for  $L_2$ . The proton beam, propagating

in the z-direction, was then intersected with a very cold ( $T \approx 1\text{-}2\text{ K}$ ) neutral  $\text{H}_2$  beam, propagating in the y-direction, from a supersonic gas jet.

Protons which were not charge-exchanged in the collision with the target were selected by a switching magnet and energy-analyzed by an electrostatic parallel-plate analyzer [24]. The projectiles which suffered an energy loss of  $\varepsilon = 57\text{ eV}$  were detected by a position-sensitive channel-plate detector. The position in the x-direction, i.e. the horizontal component, determines the scattering angle and thereby the x-component of the momentum transfer  $\mathbf{q}$ . Because of the very narrow width of the entrance and exit slits of the analyzer in the y-direction ( $75\text{ }\mu\text{m}$ )  $q_y = 0$  within the experimental resolution. The z-component of  $\mathbf{q}$  is to a very good approximation given by  $q_z = \varepsilon/v_p$ .

The recoiling  $\text{H}_2^+$  ions produced in the collisions with the projectiles were extracted by a weak and uniform electric field of  $8\text{ V/cm}$  pointing in the x-direction, then drifted in a field-free region twice as long as the extraction region, and were detected by a two-dimensional position-sensitive channel-plate detector. The recoil-ion and projectile detectors were set in coincidence. From the position information the y- and z-components of the recoil-ion momentum  $\mathbf{p}_{\text{rec}}$  could be determined. The z-component was obtained from the time-of-flight from the collision region to the detector which, in turn, is contained in the coincidence time. Finally, the ejected electron momentum was deduced by  $\mathbf{p}_{\text{el}} = \mathbf{q} - \mathbf{p}_{\text{rec}}$  using momentum conservation.

## Results and Discussions

In analogy to classical optics the cross section for a coherent beam  $d\sigma_{\text{coh}}$  can be expressed as a product of the cross section for an incoherent beam  $d\sigma_{\text{inc}}$  and the interference term  $I$ .

In other words,  $I$  is given by the ratio  $R = d\sigma_{\text{coh}}/d\sigma_{\text{inc}}$ , which is plotted for  $\varepsilon = 57$  eV as a function of the projectile scattering angle  $\theta$  in figure 1. Earlier, we attempted to extract the interference term as a ratio between the experimental cross sections (taken for a coherent beam) and twice the theoretical cross sections for ionization of atomic hydrogen  $d\sigma_{\text{H}}$  [17]. Later, large discrepancies between the theoretical and experimental  $d\sigma_{\text{H}}$  were found [25] so that twice the theoretical values do not represent a good approximation for  $d\sigma_{\text{inc}}$ . As a result these ratios from [17] do not resemble at all those plotted in figure 1. This comparison illustrates the importance of directly measuring the incoherent cross sections for obtaining reliable information about the interference term.

The  $\theta$ -dependence of  $R$  plotted in figure 1 is not constant indicating that some kind of interference is present in the coherent cross sections with a phase angle which depends on  $q_x = p_0 \sin\theta$ . Earlier, we demonstrated that FDCS ratios as a function of  $q_x$  can be well described under the assumption that interference is dominated by single-center interference with a  $q_x$ -dependent phase angle [18, 19]. It is therefore reasonable to assume that the structure in  $R(\theta)$  of figure 1 is due to the same type of interference. On the other hand the structure is much less pronounced than in the corresponding ratios for  $\varepsilon = 30$  eV [23]. This is consistent with the observation in [17] that interference structures in double differential cross sections for  $\varepsilon = 57$  eV as a function of  $\theta$  are much weaker, if present at all, than for  $\varepsilon = 30$  eV. In [19] we also reported signatures of two-center interference in the  $p_{\text{rec}}$ -dependent FDCS ratios for  $\varepsilon = 57$  eV, however, they were not observed in the  $q_x$ -dependence of these ratios.

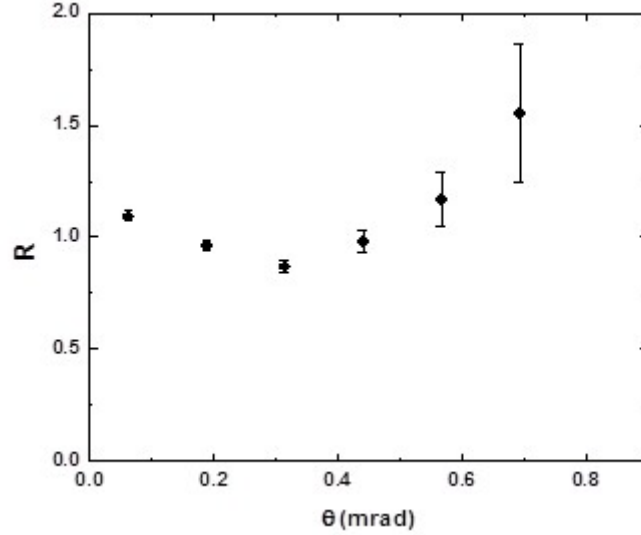


Figure 1. Ratio  $R$  between the double differential cross sections for coherent and incoherent projectile beams for a fixed energy loss of 57 eV as a function of scattering angle.

In the following we will discuss to what extent there may be a link between the apparent disappearance of interference structures in the DDCS at  $\varepsilon = 57$  eV and PCI, as contemplated in [17]. To this end we analyzed the ratios of figure 1 with additional kinematic conditions suitable to either enhance or suppress the effect of PCI on the reaction dynamics. For positively charged ion impact PCI has a tendency of focusing the ejected electrons in the forward direction. Since  $\varepsilon = 57$  eV corresponds to an electron speed which is almost the same as the projectile speed, one would therefore expect that in the longitudinal electron momentum spectrum (plotted in the top panel of figure 2 for the coherent beam) PCI leads to an enhancement of the intensity near  $p_{ez} \approx v_p$  (indicated by the vertical dashed line in figure 2). This is indeed confirmed by the top panel of figure 2, where a pronounced maximum is seen at  $p_{ez} \approx v_p$ . In the longitudinal recoil-ion momentum spectrum, shown in the bottom panel of figure 2,  $p_{ez} \approx v_p$  corresponds to  $p_{rz} = q_z - p_{ez} \approx \varepsilon/v_p - v_p = -0.54$  a.u., which again is indicated by a dashed vertical line. Here, too, a pronounced

maximum is observed at this value of  $p_{rz}$ . Therefore, it should be possible to enhance the effect of PCI on R by setting a condition on  $p_{rz}$  near  $-0.54$  a.u. and to suppress PCI by setting a condition near significantly more positive values of  $p_{rz}$ .<sup>1</sup>

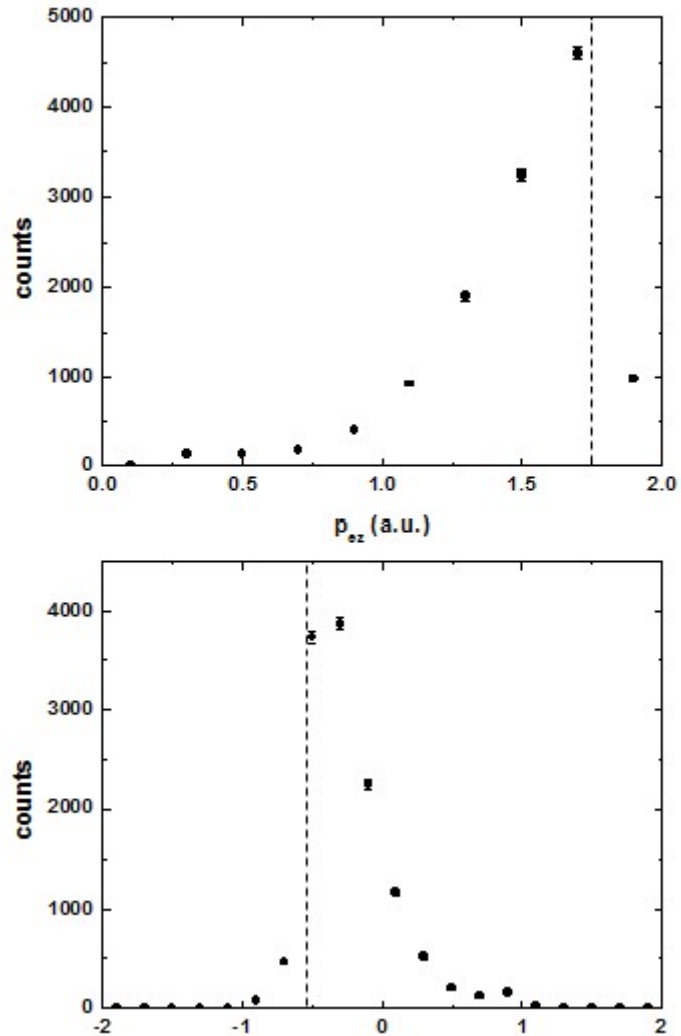


Figure 2. Longitudinal momentum spectrum for the ejected electrons (top panel) and the recoiling target ions (bottom panel). The vertical dashed lines indicate  $p_{ez} = v_p$  and  $p_{rz} = \epsilon/v_p - v_p$ , respectively.

<sup>1</sup> The same effect could be achieved by setting conditions on  $p_{ez}$  instead; however, we chose to apply these conditions to  $p_{rz}$  because it is the directly measured quantity while  $p_{ez}$  is calculated from  $p_{rz}$  and  $q_z$  using momentum conservation. Therefore the resolution is slightly better in  $p_{rz}$ .

In figure 3 the ratio between the cross sections with a condition on  $p_{rz} = -1.0$  to  $-0.1$  a.u. (to which we refer as the “PCI on” condition) and the cross sections with a condition on  $p_{rz} = -0.1$  to  $1.0$  a.u. (“PCI off” condition) is plotted as a function of  $\theta$  for the coherent beam. It can clearly be seen that the “PCI on” condition strongly favors small scattering angles, which is exactly the behavior expected for PCI [21]. This can be explained in terms of a focusing effect due to PCI, in which the scattered projectile and the ejected electron attract each other towards the initial beam axis. At  $\theta$  larger than approximately 0.4 mrad, on the other hand, the cross sections for “PCI off” become larger than for “PCI on”. This illustrates that indeed a condition on the longitudinal recoil-ion momentum is an effective method to either enhance or suppress effects due to PCI.

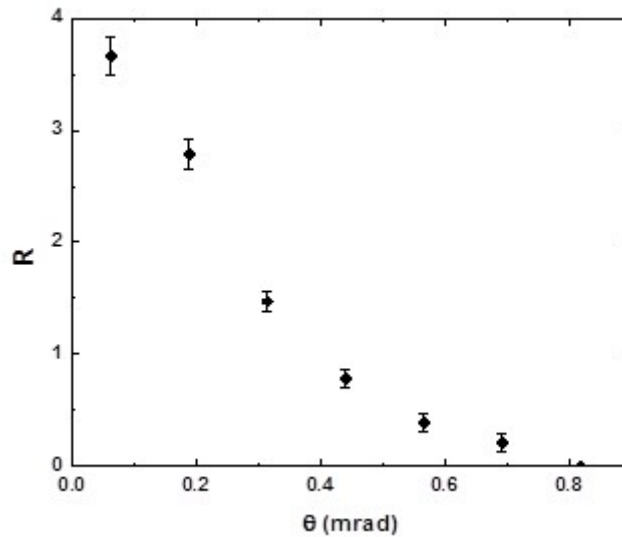


Figure 3. Ratio between the cross sections with a condition on  $p_{rz} = -1.0$  to  $-0.1$  a.u. and the cross sections with a condition on  $p_{rz} = -0.1$  to  $1.0$  a.u. as a function of scattering angle for a fixed energy loss of 57 eV and taken for the coherent projectile beam.

In figure 4 we present the ratios between cross sections measured with a coherent and incoherent beams with the “PCI on” condition (closed symbols) and the “PCI off” condition (open symbols) as a function of  $\theta$ . The “PCI on” ratios look very similar to those without any condition on  $p_{rz}$  plotted in figure 1. This is not surprising considering that the majority of events contained in figure 1 lie within the “PCI on” condition. The  $\theta$ -dependence of the “PCI off” ratios, on the other hand, is quite different. More specifically, the interference minimum, seen at about 0.3 mrad in the “PCI on” case, is shifted to 0.5 – 0.6 mrad.

In order to test our hypothesis of [17], that interference may be suppressed by a loss of coherence caused by PCI, we need to quantify how pronounced the interference structure is for the “PCI on” condition compared to the “PCI off” condition. To this end we fitted the ratios plotted in figure 4 by the model interference term, given by  $I = 1 + \alpha \cos(q_x \Delta b)$ , which we reported for single-center interference in [26], using  $\alpha$  and  $\Delta b$  as fitting parameters. Here,  $\Delta b$  is the impact parameter separation between the interfering amplitudes and  $\alpha$  describes the damping of the interference structure by incomplete coherence or experimental resolution effects. For the “PCI on” condition the best fit to the measured ratios (solid curve in figure 4) yields  $\alpha = 0.2$  and  $\Delta b = 3.5$  a.u. while for the “PCI off” condition we obtain  $\alpha = 0.3$  and  $\Delta b = 2$  a.u. (dashed curve in figure 4).

This difference in  $\alpha$  seems to support the hypothesis of [17] under consideration. However, for two reasons conclusions should be drawn cautiously. First, the fitting parameters are obviously afflicted with experimental uncertainties and it is thus not clear exactly how large the difference in  $\alpha$  is. Second, even for the “PCI off” condition  $\alpha$  is significantly smaller than for the measured ratios for  $\varepsilon = 30$  eV ( $\alpha = 0.45$ ), which are



compared in figure 5 (open symbols) to the “PCI off” ratios for  $\varepsilon = 57$  eV (closed symbols). Therefore, even if the difference in  $\alpha$  for the “PCI on” and “PCI off” conditions is as large as suggested by the results of our fitting routine it seems likely that PCI is not the only factor leading to the damping of the interference structure. On the other hand, it is certainly fair to state that the present data are not inconsistent with the hypothesis of [17] in so far as they provide some support that PCI contributes to the damping of the interference structure.

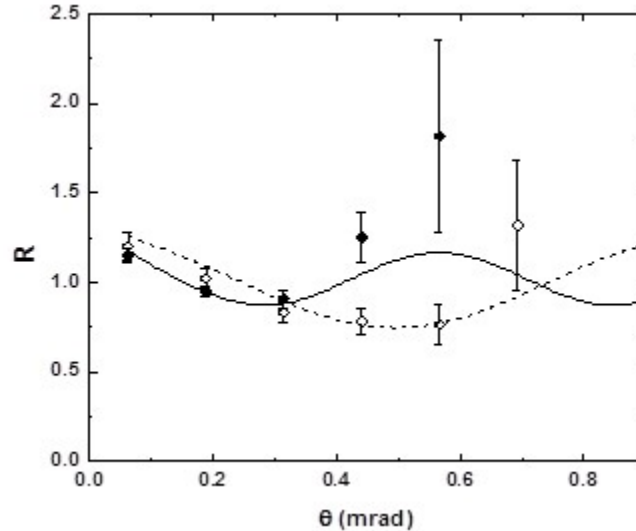


Figure 4. Same as figure 1, but with the additional condition  $p_{rz} = -1.0$  to  $-0.1$  a.u. (closed symbols) and  $p_{rz} = -0.1$  to  $1.0$  a.u. (open symbols). The dashed and solid lines are best fits of the single-center interference term to the measured ratios.

Apart from the different damping in the ratios for  $\varepsilon = 30$  eV and the “PCI off” data for  $\varepsilon = 57$  eV the shape of the  $\theta$ -dependence of both data sets in figure 5 is remarkably similar. More specifically, the period and position of the extrema in the interference oscillation are the same and fitting the ratios by the model interference term yields the same

value of  $\Delta b$  (2 a.u.). This similarity provides a clue for what else, apart from PCI, may contribute to the larger damping of the interference structure at  $\varepsilon = 57$  eV (“PCI off”) compared to  $\varepsilon = 30$  eV. It suggests that for both  $\varepsilon$  the same transition amplitudes (in e.g. a perturbation expansion) interfere with each other, although we cannot entirely rule out that different transition amplitudes could coincidentally yield the same  $\Delta b$ . However, the relative importance of the interfering amplitudes is likely to change. For example, increasing the ejected electron energy presumably requires increasingly closer collisions between the projectile and the electron. The interaction of the projectile with the target nucleus then has a smaller effect. Therefore, one might expect that the importance of the first-order amplitude, relative to higher-order amplitudes involving the nucleus-nucleus interaction, increases with increasing electron energy. Since the present collision system corresponds to a relatively large perturbation parameter  $q_p/v_p \approx 0.6$ , at small electron energies the higher-order amplitudes could be of similar magnitude as the first-order amplitudes, which is a favorable condition for pronounced interference structures. At larger electron energies, on the other hand, the higher-order amplitudes could be substantially smaller leading to a damping of the interference structure.

The additional damping of the interference structure for the “PCI on” condition, relative to the “PCI off” condition”, might be due to the coherence properties of the projectile beam with respect to  $\Delta b$ . In the comparison between  $\varepsilon = 57$  eV (“PCI off”) and  $\varepsilon = 30$  eV this does not play any role because both  $\Delta x$  and  $\Delta b$  are identical for both cases. But for the “PCI on” condition our fit of the model interference term to the measured ratios yields  $\Delta b$  similar to  $\Delta x$  so that the beam is only marginally coherent (although the observation of a residual interference structure shows that the beam is not completely

incoherent yet). At present, we cannot explain why  $\Delta b$  is significantly larger for the “PCI on” condition. PCI is a rather complex process which in some sense goes beyond second order. This can be understood using a classical analogy: After two particles collided with each other they cannot collide for a second time, because they depart from each other, unless one of them gets redirected by an interaction with a third particle. In the case of PCI that third particle is the target nucleus, which can redirect either the electron or the projectile. Another complication is that  $\Delta b$  is measured in three-dimensional space. For example, the ionization process may be selective on impact parameter vectors pointing in opposite directions for the interfering amplitudes under some kinematic conditions, but in

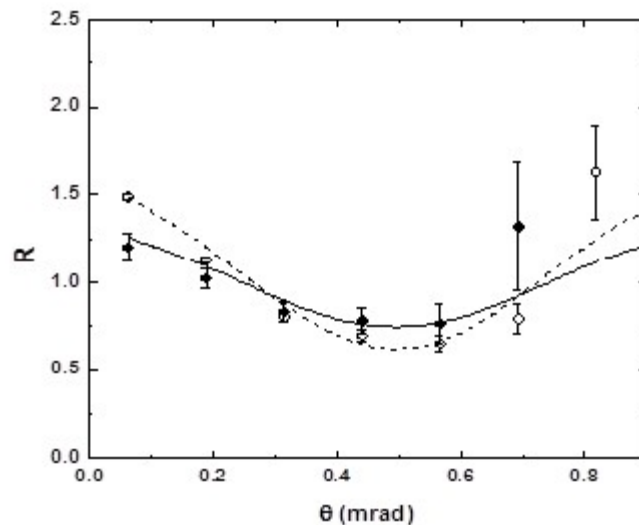


Figure 5. Ratio  $R$  between the double differential cross sections for coherent and incoherent projectile beams for a fixed energy loss of 30 eV (open symbols) and of 57 eV with the additional condition  $p_{rz} = -0.1$  to 1.0 a.u. as a function of scattering angle. The dashed and solid lines are best fits of the single-center interference term to the measured ratios.

the same direction for other conditions. It is therefore not easy to make even a qualitative prediction as to how  $\Delta b$  should depend on the relative importance of PCI without elaborate

theoretical calculations. In particular, calculations of impact parameter dependent transition amplitudes for first- and higher order contributions would be very helpful in interpreting the data.

## Conclusions

We have presented a kinematically complete experimental study of interference effects in ionization of  $H_2$  by intermediate energy proton impact for electrons emitted with a speed equal to the projectile speed. Several years ago, we observed that for this electron energy interference structures in the projectile scattering angle dependence of the ionization cross sections were significantly less pronounced than at smaller electron energies [17]. More recently we demonstrated that single-center and molecular two – center interference can experimentally be separated [19]. Furthermore, in that work we found scattering-angle dependent cross sections are dominated by single-center interference and recoil-ion momentum dependent cross sections by molecular two-center interference. Considering the combination of the results obtained from [17] and [19] it was the aim of the present study to better understand a potential link between single-center interference and the post-collision interaction (PCI), which is known to be very important for ejected electron speeds close to the projectile speed.

We demonstrated that setting a condition on the longitudinal recoil-ion momentum is an effective method to either enhance (by selecting ions recoiling in the backward direction) or to suppress (by selecting all other recoil ions) effects due to PCI. Thereby we were able to analyze the interference term for a given electron speed (here  $v_e = v_p$ ) under conditions of weak or strong PCI. Our present results confirm our earlier observation [17]

that, independent of whether PCI is weak or strong, interference is less pronounced than at smaller electron energies. A possible explanation, calling for theoretical confirmation, is that for small electron energies the interfering amplitudes may be of similar magnitude (due to the large perturbation parameter) while for larger electron energies the first-order amplitude may be significantly larger. In addition, for strong PCI the interference structure is even less pronounced than for weak PCI. Furthermore, in the former case the impact parameter separation between the interfering amplitudes is significantly larger than in the latter case, for which it is essentially the same as for small electron energies. Therefore the fixed coherence length corresponds to a less coherent projectile beam for strong PCI and a more coherent beam for weak PCI. This offers a plausible explanation for the stronger damping of the interference structure in the case of strong PCI. However, explaining the larger impact parameter separation for this case has to await further theoretical analysis.

### **Acknowledgements**

This work was supported by the National Science Foundation under grant no. PHY 1401586.

### **References**

- [1] M. Schulz, R. Moshhammer, D. Fischer, H. Kollmus, D.H. Madison, S. Jones, and J. Ullrich, *Nature* 422, 48 (2003).
- [2] M. Schulz, R. Moshhammer, A.N. Perumal, and J. Ullrich, *J. Phys. B* 35, L161 (2002).
- [3] N.V. Maydanyuk, A. Hasan, M. Foster, B. Tooke, E. Nanni, D.H. Madison, and M.Schulz, *Phys. Rev. Lett.* 94, 243201 (2005).

- [4] M. Schulz, B. Najjari, A.B. Voitkiv, K. Schneider, X. Wang, A.C. Laforge, R. Hubele, J. Goullon, N. Ferreira, A. Kelkar, M. Grieser, R. Moshhammer, J. Ullrich, and D. Fischer, *Phys. Rev. A* 88, 022704 (2013).
- [5] R. Hubele, A.C. Laforge, M. Schulz, J. Goullon, X. Wang, B. Najjari, N. Ferreira, M. Grieser, V.L.B. de Jesus, R. Moshhammer, K. Schneider, A.B. Voitkiv, and D. Fischer, *Phys. Rev. Lett.* 110, 133201 (2013).
- [6] M. Schulz and D.H. Madison, *International Journal of Modern Physics A* 21, 3649 (2006).
- [7] D. Madison, M. Schulz, S. Jones, M. Foster, R. Moshhammer, and J. Ullrich, *J. Phys. B* 35, 3297 (2002).
- [8] M.F. Ciappina, W.R. Cravero, and M. Schulz, *J. Phys. B* 40, 2577 (2007).
- [9] A.B. Voitkiv, B. Najjari, and J. Ullrich, *J. Phys. B* 36, 2591 (2003).
- [10] M. McGovern, C.T. Whelan, and H.R.J. Walters, *Phys. Rev. A* 82, 032702 (2010).
- [11] J. Colgan, M.S. Pindzola, F. Robicheaux, and M.F. Ciappina, *J. Phys. B* 44, 175205 (2011).
- [12] K.A. Kouzakov, S.A. Zaytsev, Yu.V. Popov, and M. Takahashi, *Phys. Rev. A* 86, 032710 (2012).
- [13] X.Y. Ma, X. Li, S.Y. Sun, and X.F. Jia, *Europhys. Lett.* 98, 53001 (2012).
- [14] R.T. Pedlow, S.F.C. O'Rourke, and D.S.F. Crothers, *Phys. Rev. A* 72, 062719 (2005).
- [15] N. Stolterfoht, B. Sulik, V. Hoffmann, B. Skogvall, J.Y. Chesnel, J. Ragnama, F. Frémont, D. Hennecart, A. Cassimi, X. Husson, A.L. Landers, J. Tanis, M.E. Galassi, and R.D. Rivarola, *Phys. Rev. Lett.* 87, 23201 (2001).
- [16] D. Misra, A. Kelkar, U. Kadhane, A. Kumar, L.C. Tribedi, and P.D. Fainstein, *Phys. Rev. A* 74, 060701 (2006).
- [17] J.S. Alexander, A.C. Laforge, A. Hasan, Z.S. Machavariani, M.F. Ciappina, R.D. Rivarola, D.H. Madison, and M. Schulz, *Phys. Rev. A* 78, 060701 (2008).
- [18] S. Sharma, T.P. Arthanayaka, A. Hasan, B.R. Lamichhane, J. Remolina, A. Smith, and M. Schulz, *Phys. Rev. A* 90, 052710 (2014).
- [19] T.P. Arthanayaka, S. Sharma, B.R. Lamichhane, A. Hasan, J. Remolina, S. Gurung, and M. Schulz, *J. Phys. B* 48, 071001 (2015).

- [20] A. Salin, *J. Phys. B* 2, 631 (1969).
- [21] T. Vajnai, A.D. Gaus, J.A. Brand, W. Htwe, D.H. Madison, R.E. Olson, J.L. Peacher, and M. Schulz, *Phys. Rev. Lett.* 74, 3588 (1995).
- [22] A. Hasan, S. Sharma, T.P. Arthanayaka, B.R. Lamichhane, J. Remolina, S. Akula, D.H. Madison, and M. Schulz, *J. Phys. B* 47, 215201 (2014).
- [23] K.N. Egodapitiya, S. Sharma, A. Hasan, A.C. Laforge, D.H. Madison, R. Moshhammer, and M. Schulz, *Phys. Rev. Lett.* 106, 153202 (2011).
- [24] A.D. Gaus, W. Htwe, J.A. Brand, T.J. Gay, and M. Schulz, *Rev. Sci. Instrum.* 65, 3739 (1994).
- [25] A.C. Laforge, K.N. Egodapitiya, J.S. Alexander, A. Hasan, M.F. Ciappina, M.A. Khakoo, and M. Schulz, *Phys. Rev. Lett.* 103, 053201 (2009).
- [26] S. Sharma, T.P. Arthanayaka, A. Hasan, B.R. Lamichhane, J. Remolina, A. Smith, and M. Schulz, *Phys. Rev. A* 89, 052703 (2014).

### III. Fully differential study of ionization in $p + H_2$ collisions near electron – projectile velocity matching

A. Hasan<sup>1,2</sup>, T. Arthanayaka<sup>1</sup>, B.R. Lamichhane<sup>1</sup>, S. Sharma<sup>1</sup>, S. Gurung<sup>1</sup>, J. Remolina<sup>1</sup>,  
S. Akula<sup>1</sup>, D.H. Madison<sup>1</sup>, M.F. Ciappina<sup>3</sup>, R.D. Rivarola<sup>4</sup>, and M. Schulz<sup>1</sup>

<sup>1</sup>Dept. of Physics and LAMOR, Missouri University of Science & Technology, Rolla,  
MO 65409

<sup>2</sup>Dept. of Physics, UAE University, P.O. Box 15551, Al Ain, Abu Dhabi, UAE

<sup>3</sup>Max Planck Institute of Quantum Optics, Hans-Kopfermann Str. 1, D-85748 Garching,  
Germany

<sup>4</sup>Laboratorio de Colisiones Atómicas, Instituto de Física Rosario, CONICET y  
Universidad Nacional de  
Rosario, Bv. 27 de Febrero 210 bis, 2000 Rosario, Argentina

#### Abstract

We have performed a kinematically complete experiment on ionization of  $H_2$  by 75 keV proton impact for electrons ejected with a speed close to the projectile speed. The fully differential data are compared to a three-body distorted wave and a continuum distorted wave – eikonal initial state calculation. Large discrepancies between experiment and theory, as well as between both calculations, are found. These probably arise from a strong coupling between the ionization and capture channels, which is not accounted for by theory.



## Introduction

With the advent of cold target recoil ion momentum spectroscopy (COLTRIMS [1,2]) kinematically complete experiments on target ionization by ion impact became feasible [3,4]. In this method, the recoil-ion momentum is measured in addition to the momentum of either the ejected electron [e.g. 5-9] or the scattered projectile [e.g. 10-13] and the momentum of the third (undetected) collision fragment is obtained using momentum conservation. The fully differential cross sections (FDCS) that can be extracted from such experiments offer the most sensitive tests of theoretical models (for a recent review see [14]).

Initially, these experiments focused on studying ionization of helium [e.g. 5-7,9,10]. After theory had made remarkable progress in reproducing experimental data for ionization of simple targets by electron impact [e.g. 15,16], it was quite surprising that for ion impact significant, in some cases severe, discrepancies were found [e.g. 17-22]. Recently, an experimental study [23] suggested that these discrepancies may be partly due to the projectile coherence properties, which are not realistically treated in most of the existing theoretical models. For fast heavy ions the coherence length tends to be very small so that only a small fraction of the target dimension is coherently illuminated. As a result, interference effects, present in calculations assuming a coherent projectile beam, are not experimentally observable. This interpretation has since received further experimental support [11, 13, 24, and 25]. Nevertheless, especially for highly-charged ion impact, it seems likely that the projectile coherence properties are not the only factor contributing to the discrepancies. For this ion species, higher-order contributions to the transition

amplitudes can reach a magnitude large enough to represent an enormous challenge to theory.

Higher-order processes involving the post-collision interaction (PCI) between the outgoing scattered projectile and the electron, which has been lifted to the continuum by a preceding primary interaction, have been studied extensively [e.g. 6,9,26-29]. These studies have shown that the role of PCI maximizes when the electron speed  $v_{el}$  approaches the projectile speed  $v_p$  [29,30]. Well-known manifestations of the PCI are the occurrence of a sharp peak in the energy spectrum (the so-called cusp peak) of electrons ejected in the forward direction [26-28] and a narrowing of the scattered projectile angular distribution, which is particularly pronounced when  $v_{el} \approx v_p$  [29]. However, FDCS are very difficult to measure for this kinematic regime, at least for fast-ion impact. The problem is that for projectile energies of the order of MeV/amu  $v_{el} \approx v_p$  corresponds to ejected electron energies of the order of keVs. To directly measure such large electron energies within a COLTRIMS set-up is only possible at the expense of a poor recoil-ion momentum resolution. The only experimental FDCS for  $v_{el} \approx v_p$  reported so far were measured for 75 keV  $p + H_2$  collisions [13], for which the corresponding electron energy is relatively small (41.6 eV). Furthermore, the electron energy was not measured directly, but obtained from the projectile energy loss. That work was focused on the role of projectile coherence effects; impacts of the PCI on the collision dynamics were not analyzed.

In this communication we present the first comparative study between experiment and theory on FDCS for ionization of  $H_2$  by ion impact in the regime  $v_{el} \approx v_p$ , which is still a largely unexplored kinematic regime. The measurements and calculations were performed for various electron ejection geometries. Stunning discrepancies not only

between the measured and calculated FDCS, but also between two conceptually similar theoretical models were found. This indicates a large sensitivity of the FDCS to the details of the dynamics of the ionization process for  $v_{el} \approx v_p$ . A strong coupling between the ionization and capture channels in this regime could at least partly be responsible for these unusual discrepancies.

## Experiment

The details of the experiment have been reported previously [11, 12]. In brief: a proton beam was extracted from a hot cathode ion source and accelerated to an energy of 75 keV plus 57 eV. The beam was collimated by an aperture 1.5 mm in diameter, located at the end of the accelerator terminal, and by a pair of horizontal and vertical slits with a width of 150  $\mu\text{m}$  placed at a distance of 50 cm before the target region. This geometry of the collimating slit corresponds to a transverse coherence length of about 3.3 a.u. After intersecting a very cold ( $T \approx 1 - 2$  K) neutral  $\text{H}_2$  target beam the projectiles passed through a switching magnet to eliminate charge-exchanged beam components.

The protons were then decelerated by 70 keV and energy-analyzed by an electrostatic parallel-plate analyzer [31] (for a review on projectile energy-loss spectroscopy see [32]), which was set to a pass-energy of 5 keV. Therefore, only protons which suffered an energy loss of  $\varepsilon = 57$  eV in the collision with the target passed the analyzer and were detected by a two-dimensional position-sensitive micro-channel plate detector. The entrance and exit slits were very narrow (75  $\mu\text{m}$ ) in the vertical direction ( $y$ -direction) and long ( $\approx 2.5$  cm) in the  $x$ -direction. Therefore, the  $y$ -component of the momentum transfer  $\mathbf{q} = \mathbf{p}_o - \mathbf{p}_f$  (where  $\mathbf{p}_o$  and  $\mathbf{p}_f$  are the initial and final projectile momenta)

was fixed at zero (within the resolution) and the x-component could be determined from the x-component of the position on the detector. The scattering angle  $\theta_p = \sin^{-1}(q_x/p_o)$  was obtained with a resolution of about 0.13 mrad full width at half maximum (FWHM). The z-component of  $\mathbf{q}$  is to a very good approximation given by  $q_z = \varepsilon/v_p = 1.21$  a.u.. The energy loss resolution of 3 eV FWHM corresponds to a resolution in  $q_z$  of 0.06 a.u. FWHM.

The  $\text{H}_2^+$  recoil ions produced in the collision were extracted by a weak, nearly uniform electric field ( $E \approx 8\text{V/cm}$ ) pointing in the x-direction applied over a length of 5 cm. The ions then drifted in a field free region 10 cm in length and were finally detected by a second two-dimensional position-sensitive micro-channel plate detector. From the position information the two momentum components in the plane of the detector (i.e. the y- and z-components) could be determined. The projectile and recoil-ion detectors were set in coincidence. The time-of-flight of the recoil ions from the collision region to the detector, which is contained in the coincidence time, was used to calculate the x-component of the recoil-ion momentum vector. The resolution in the x-, y-, and z-components was 0.15, 0.5, and 0.15 a.u. FWHM, respectively. The electron momentum was obtained using momentum conservation as  $\mathbf{p}_{el} = \mathbf{q} - \mathbf{p}_{rec}$ .

## Results and Discussions

The experimental results are compared with the molecular continuum distorted wave Eikonal initial state approximation (CDW-EIS MO) [33] and the molecular three-body distorted wave Eikonal initial state (M3DW-EIS) approximation [34] which have been described in previous publications, so only a brief description noting the similarities and differences will be presented here. In the CDW-EIS MO approach [33], the T-matrix is

approximated as a sum of two terms corresponding to ionization of effective atomic wavefunctions centered on the two  $H_2$  nuclei. CDW-EIS transition amplitudes are used for the individual atomic terms within an impact parameter approximation. This approximation allows treating separately the quantum-mechanical dynamics of the electrons from the classical dynamics of the nuclei. Then, the interaction between the projectile and the target nuclei, the so-called N-N interaction, is considered in all orders within this approximation. The average over all molecular orientations yields a cross section which is a product of an interference term and a CDW-EIS cross section for the two effective atomic centers.

The M3DW-EIS approach [34] is a fully quantum mechanical approach with the initial projectile wave-function being represented as an Eikonal wave and the scattered projectile being represented as a Coulomb wave for effective charge +1. The initial molecular wave-function is represented by a numerical Hartree-Fock  $H_2$  ground state Dyson orbital averaged over all orientations. The ejected electron wave-function is a numerical distorted wave calculated using a two-center distorting potential obtained from the Hartree-Fock  $H_2$  charge density averaged over all orientations. The final state wave-function for the system is approximated as a product of the Coulomb wave for the projectile, the distorted wave for the ejected electron and the exact final state projectile-electron interaction (PCI). Finally, the initial state projectile-target interaction contains both the projectile-active electron interaction and the interaction between the projectile and an effective ion of charge +1.

In figure 1 the FDCS are plotted for electrons with an energy of 41.6 eV ejected into the scattering plane, spanned by  $\mathbf{p}_0$  and  $\mathbf{q}$ , as a function of the polar electron ejection

angle  $\theta_{el}$ .  $\theta_p$  was fixed at 0.1 mrad (upper left panel), 0.2 mrad (upper right panel), 0.325 mrad (lower left panel), and 0.55 mrad (lower right panel), respectively. The arrows indicate the direction of the momentum transfer for each  $\theta_p$ . In the experimental data, in each case a pronounced peak structure, the so-called binary peak, is observed near the direction of  $\mathbf{q}$ . With increasing  $\theta_p$  the binary peak is increasingly shifted in the forward direction relative to  $\mathbf{q}$ . A similar trend was also observed in the FDCS for ionization by fast highly charged ion impact [9].

The solid and dashed curves in figure 1 show calculations based on the molecular 3-body distorted wave-Eikonal initial state (M3DW-EIS) [34] and the continuum distorted wave – Eikonal initial state (CDW-EIS) [33] approaches, respectively. As described above, the two models represent different approximations for essentially the same physics. Although both of them treat the ionization process perturbatively to first order in the operator of the T-matrix, they both also incorporate higher-order contributions (both in the projectile - electron and in the projectile - target nucleus interaction) in the final-state wavefunction. Although the results of both models are qualitatively similar, dramatic discrepancies to the experimental data are quite obvious: In both calculations a very sharp and large peak structure is found at  $\theta_{el} = 0$  for all scattering angles, which is absent in the measured FDCS. Furthermore, the binary peak, i.e. the only structure observed in the experimental data, is completely missing in both calculations for  $\theta_p = 0.1$  mrad. For all  $\theta_p$  the height of the  $0^\circ$  peak in the calculations is much larger than the magnitude of the binary peak in the experimental FDCS (for  $\theta_p = 0.1$  mrad by about an order of magnitude in case of the M3DW-EIS results). Considering the conceptual similarity between both models, the large differences in magnitudes between the two theoretical curves are quite surprising.

On the other hand, for the two larger  $\theta_p$ , the shape of the measured binary peak is very well reproduced by both calculations and for  $\theta_p = 0.325$  mrad, the M3DW-EIS model also predicts the magnitude correctly.

A strong  $0^\circ$  peak for  $v_{el} = v_p$  appears to be a feature which one may have expected since the attractive PCI is known to produce an enhanced electron flux in the forward direction. This may raise the question whether the discrepancies between experiment and theory are simply due to inaccuracies in the calibration shifting the peak, which should be located at  $0^\circ$ , to larger  $\theta_{el}$ . However, this could not explain the comparison between experiment and theory at the two larger  $\theta_p$ , where in the calculations two peak structures are observed, but only one in the measured FDCS. Furthermore, the accuracy of the calibration has been thoroughly tested [35] and also seems to be confirmed by the good agreement between experiment and theory regarding the location of the binary peak. Finally, we found that the shape of the FDCS near  $\theta_{el} = 0$  is surprisingly insensitive to the calibration.

Another possibility is that the absence of the  $0^\circ$  peak in the data could be due to its very small width ( $6^\circ$  FWHM in the CDW-EIS calculation). Since data points are taken in steps of  $10^\circ$  the peak structure could simply be “missed”. However, the angular resolution ( $\approx 15^\circ$  FWHM) is larger than the step size so that the  $0^\circ$  peak should have been observed, although with a much larger width than in the calculation and therefore, since the integrated peak content cannot change, with a reduced height. That leaves the possibility that the  $0^\circ$  peak is not resolved from the binary peak and/or so much reduced in height because of the resolution that it is no longer visible. We have therefore convoluted the CDW-EIS calculation for  $\theta_p = 0.325$  mrad with a pessimistic resolution of  $20^\circ$  FWHM and the result

is shown, after renormalizing to the height of the experimental binary peak, as the dotted curve in figure 1. Indeed, in the convolution the height of the  $0^\circ$  peak is significantly reduced relative to the binary peak, but nevertheless a well-resolved structure as tall as the binary peak remains. A further increase in resolution would make the binary peak too broad compared to the experimental data. We therefore conclude that the poor agreement between the measured and calculated FDCS cannot be explained by experimental artifacts, at least not for the two larger  $\theta_p$ . For  $\theta_p = 0.1$  mrad (and possibly also for 0.2 mrad), on the other hand, it is quite possible that a significant  $0^\circ$  peak, unresolved from the binary peak, exists in the experimental data. But even if this is the case, the magnitude of the  $0^\circ$  peak relative to the binary peak would still be severely overestimated by theory since the maximum in the measured FDCS is much closer to the direction of  $\mathbf{q}$  than to  $0^\circ$ .

Some discrepancies between experiment and the M3DW-EIS model, although not nearly as large as in the present study, was also found in the FDCS for  $\varepsilon = 30$  eV [12]. In that work we considered the possibility that the capture channel, which is not accounted for in the calculation, may be responsible at least for part of the discrepancies. Electrons promoted to the continuum by a primary interaction with the projectile can eventually get captured to the projectile by subsequent interactions. However, the theoretical model does not contain bound projectile states and all electrons removed from the target therefore must remain in the continuum. The capture probability steeply increases with decreasing relative velocity between the electron and the projectile. For  $\mathbf{v}_{el} \approx \mathbf{v}_p$  (i.e.  $\varepsilon = 57$  eV and  $\theta_{el} = 0$ ) this probability could saturate leading to a strong depletion of the FDCS for ionization in this kinematic regime. This would explain the absence of the  $0^\circ$  peak in the experimental data. In order to test this explanation a non-perturbative coupled-channel calculation, using



a two-center basis set, would be very helpful. Since such a model would account for the capture channel the  $0^\circ$  peak should be at least strongly reduced.

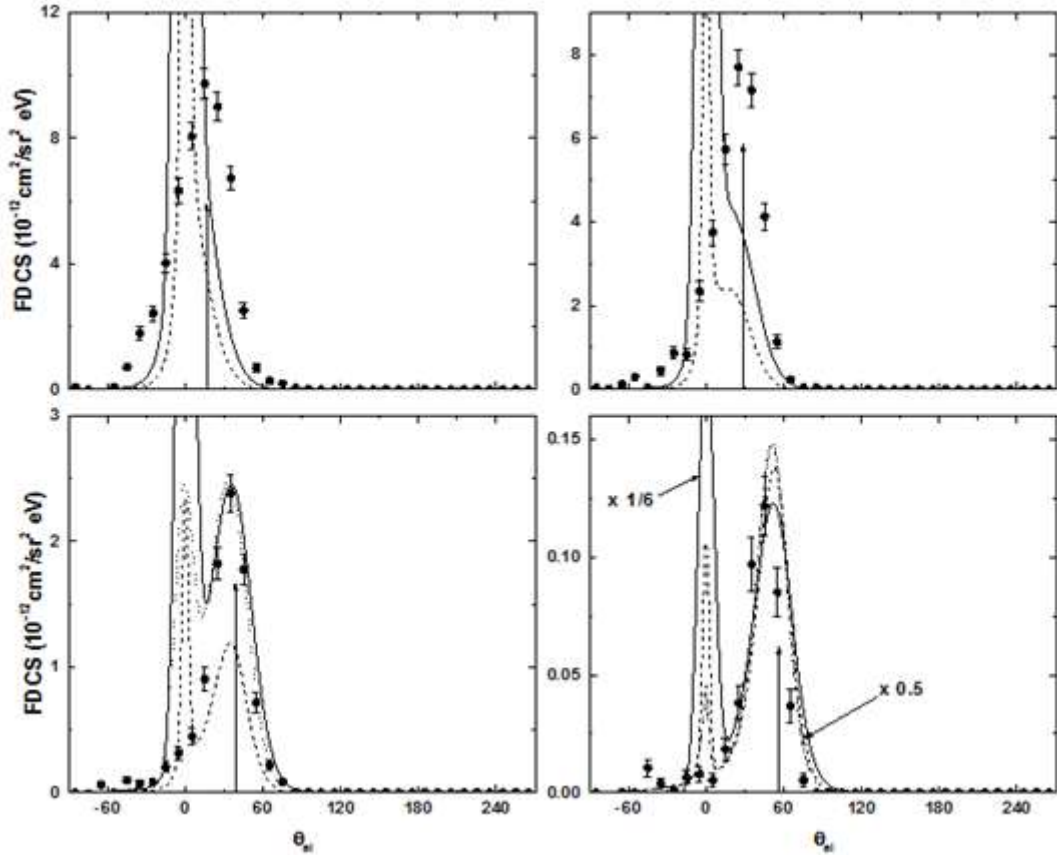


Figure 1. Fully differential cross sections for electrons with an energy of 41.6 eV ejected into the scattering plane as a function of the polar electron emission angle. The projectile scattering angle is fixed at 0.1 mrad (upper left), 0.2 mrad (upper right), 0.325 mrad (lower left), and 0.55 mrad (lower right). Solid curves, M3DW-EIS calculations; dashed curves, CDW-EIS calculations; dotted curve (for 0.325 mrad), CDW-EIS calculation convoluted with an angular resolution of  $20^\circ$  FWHM; dash-dotted curve (for 0.55 mrad), CDW-EIS calculation for an ejected electron energy of 43.6 eV.

A similar feature as in the present data, with reversed roles between experiment and theory, was found in the FDCS for 3.6 MeV/amu  $\text{Au}^{53+} + \text{He}$  collisions [6]. There, a pronounced  $0^\circ$  peak was observed in the measured FDCS in addition to the binary peak,

which was completely absent in the calculations. One important difference was that the speed of the ejected electron was much smaller than the projectile speed. Nevertheless,

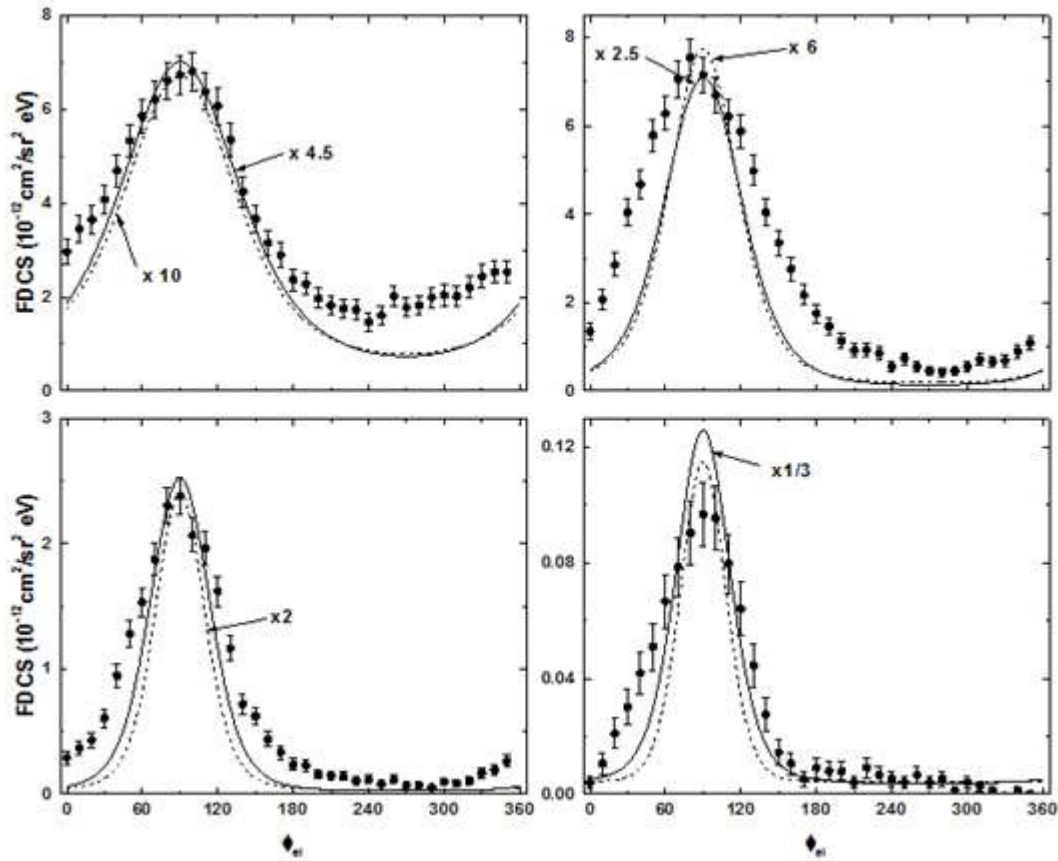


Figure 2. Fully differential cross sections for electrons with an energy of 41.6 eV ejected along the surface of a cone with an opening angle of  $35^\circ$  as a function of the azimuthal electron emission angle. The projectile scattering angle was fixed at the same values as in figure 1. Solid and dashed curves as in figure 1.

due to the very large projectile charge, PCI played a similarly important role as in the present data. However, the electron flux in the  $0^\circ$  peak probably did not get depleted as strongly by the capture channel because of the large relative speed of about 10 a.u. between the electron and the projectile. On the other hand, based on this argument, the missing capture channel in the perturbative models should not pose a serious problem and the

question arises why the  $0^\circ$  peak could not even qualitatively be reproduced by theory. We cannot offer a definite answer to this question, however, we allude to the extremely large perturbation parameter (projectile charge to speed ratio  $\approx 4.4$ ) for this collision system, for which the validity of perturbative approaches is not clear. For example, the importance of PCI may be severely underestimated.

Another possible explanation for the missing  $0^\circ$  peak in the present measured FDCS is related to a study of Shah et al, where the shape of the cusp peak was studied for low-energy  $p + H_2$  and  $p + He$  collisions [36]. They found that the cusp peak was shifted in position to an electron speed which was about 5 to 10 % smaller than  $v_p$ . They interpreted this shift as being due to a post-collisional interaction of the residual target ion with the ejected electron (to which we refer as target PCI), which acts in the opposite direction as the projectile PCI. This conclusion was disputed by Sarkadi and Barrachina [37]. They argued that the bulk of the shift can be explained by the finite acceptance angle of the electron analyzer and misalignment effects. However, to the best of our knowledge the question whether the target PCI can lead to a significant shift of the cusp peak has never been conclusively settled. In our case  $v_{el}$  is actually slightly larger than  $v_p$  (by about 1 %), which according to the data of Shah et al. would already be outside the (shifted) cusp peak. However, it should be noted that in the present study,  $v_p$  was nearly a factor of 2 larger and any shift of the cusp peak due to the target PCI should be reduced. Nevertheless, we cannot entirely rule out that the target PCI may also contribute to a suppression of the  $0^\circ$  peak.

In order to test how sensitive the shape of the FDCS is to a shift of the cusp peak we performed the CDW-EIS calculations also for  $\varepsilon = 59$  eV, which corresponds to a change in the ejected electron speed by only 2%. The results are shown in figure 1 for  $\theta_p = 0.55$

mrاد as the dash-dotted curve. Relative to  $\varepsilon = 57$  eV the  $0^\circ$  peak is reduced by almost a factor of 3, while the binary peak is slightly increased. For the other  $\theta_p$  similar differences between the FDCS for these two energy losses were found. Therefore, if the target PCI shifts the cusp peak to smaller electron energies, as asserted by Shah et al., then it could sensitively affect the shape of the FDCS for electron speeds close to the projectile speed. However, the vast overestimation of the  $0^\circ$  peak for  $\varepsilon = 57$  eV would then suggest that either the shift of the cusp peak is not accurately described by CDW-EIS or this model would probably predict an even much larger  $0^\circ$  peak at the actual cusp peak energy.

In figure 2 the FDCS are shown for fixed  $\theta_{el} = 35^\circ$  and the same values of  $\theta_p$  as in figure 1 as a function of the azimuthal electron ejection angle  $\phi_{el}$ , where  $\phi_{el} = 90^\circ$  coincides with the azimuthal angle of  $\mathbf{q}$ . Since  $\theta_{el} = 35^\circ$  is close to the polar angle of  $\mathbf{q}$ , at least for  $\theta_p = 0.2$  and  $0.325$  mrad, the data points at  $\phi_{el} = 90^\circ$  are close to the binary peak. For all  $\theta_p$  the entire data sets of figure 2 are far from the  $0^\circ$  peak predicted by theory. Therefore, for this geometry the comparison between measured and calculated FDCS (the same calculations are shown by the same curves as in figure 1) shows how well the collision dynamics is described by theory in a regime which should not be as strongly affected by the capture channel as the forward direction. Significant discrepancies, especially to the CDW-EIS calculations, are still present, but they are not as severe as in the scattering plane. For the same geometry, but an energy loss of 30 eV, the discrepancies, especially in the magnitude, were significantly smaller [12, 34]. This is a hint that even far away from the  $0^\circ$  peak the capture channel could present a problem to perturbative calculations.

## Conclusions

In summary, we have presented the first fully differential comparative study between experiment and theory on target ionization by ion impact in the regime of velocity matching of the ejected electron with the projectile. Remarkable discrepancies between experiment and theory and between two conceptually similar theoretical models were found. This indicates a large sensitivity of the cross sections to the details of the collision dynamics in this regime. A possible explanation for the discrepancies between the measured and calculated cross sections is a strong coupling between the ionization and capture channels, which is not accounted for in both theoretical models. This should be particularly important for electrons ejected to a state just above the continuum limit of the target, but our data suggest that it may still be significant far away from this regime.

## Acknowledgements

This work was supported by the National Science Foundation under grant nos. PHY-1401586 and PHY-1505819.

## References

- [1] R. Dörner, V. Mergel, O. Jagutzski, L. Spielberger, J. Ullrich, R. Moshhammer, and H. Schmidt-Böcking, *Phys. Rep.* 330, 95 (2000).
- [2] J. Ullrich, R. Moshhammer, A. Dorn, R. Dörner, L. Schmidt, and H. Schmidt-Böcking, *Rep. Prog. Phys.* 66, 1463 (2003).
- [3] R. Moshhammer, J. Ullrich, M. Unverzagt, W. Schmitt, P. Jardin, R.E. Olson, R. Mann, R. Dörner, V. Mergel, U. Buck and H. Schmidt-Böcking, *Phys. Rev. Lett.* 73, 3371 (1994).

- [4] R. Dörner, H. Khemliche, M.H. Prior, C.L. Cocke, J.A. Gary, R.E. Olson, V. Mergel, J. Ullrich, and H. Schmidt-Böcking, *Phys. Rev. Lett.* 77, 4520 (1996).
- [5] M. Schulz, R. Moshhammer, D. Fischer, H. Kollmus, D.H. Madison, S. Jones, and J. Ullrich, *Nature* 422, 48 (2003).
- [6] M. Schulz, R. Moshhammer, A.N. Perumal, and J. Ullrich, *J. Phys. B* 35, L161 (2002).
- [7] M. Schulz, R. Moshhammer, A. Voitkiv, B. Najjari, and J. Ullrich, *Nucl. Instrum. Meth. B* 235, 296 (2005).
- [8] R. Hubele, A.C. Laforge, M. Schulz, J. Goullon, X. Wang, B. Najjari, N. Ferreira, M. Grieser, V.L.B. de Jesus, R. Moshhammer, K. Schneider, A.B. Voitkiv, and D. Fischer, *Phys. Rev. Lett.* 110, 133201 (2013).
- [9] M. Schulz, B. Najjari, A.B. Voitkiv, K. Schneider, X. Wang, A.C. Laforge, R. Hubele, J. Goullon, N. Ferreira, A. Kelkar, M. Grieser, R. Moshhammer, J. Ullrich, and D. Fischer, *Phys. Rev. A* 88, 022704 (2013).
- [10] N.V. Maydanyuk, A. Hasan, M. Foster, B. Tooke, E. Nanni, D.H. Madison, and M. Schulz, *Phys. Rev. Lett.* 94, 243201 (2005).
- [11] S. Sharma, T.P. Arthanayaka, A. Hasan, B.R. Lamichhane, J. Remolina, A. Smith, and M. Schulz, *Phys. Rev. A* 90, 052710 (2014).
- [12] A. Hasan, S. Sharma, T.P. Arthanayaka, B.R. Lamichhane, J. Remolina, S. Akula, D.H. Madison, and M. Schulz, *J. Phys. B* 47, 215201 (2014).
- [13] T.P. Arthanayaka, S. Sharma, B.R. Lamichhane, A. Hasan, J. Remolina, S. Gurung, and M. Schulz, *J. Phys. B* 48, 071001 (2015).
- [14] M. Schulz and D.H. Madison, *International Journal of Modern Physics A* 21, 3649 (2006).
- [15] T.N. Rescigno, M. Baertschy, W.A. Isaacs, and C.W. McCurdy, *Science* 286, 2474 (1999).
- [16] X. Ren, I. Bray, D.V. Fursa, J. Colgan, M.S. Pindzola, T. Pflüger, A. Senftleben, S. Xu, A. Dorn, and J. Ullrich, *Phys. Rev. A* 83, 052711 (2011).
- [17] R.T. Pedlow, S.F.C. O'Rourke, and D.S.F. Crothers, *Phys. Rev. A* 72, 062719 (2005).
- [18] M.F. Ciappina, W.R. Cravero, and M. Schulz, *J. Phys. B* 40, 2577 (2007).
- [19] M. McGovern, D. Assafrão, J.R. Mohallem, C.T. Whelan, and H.R.J. Walters, *Phys. Rev. A* 81, 042704 (2010).

- [20] K.A. Kouzakov, S.A. Zaytsev, Yu.V. Popov, and M. Takahashi, *Phys. Rev. A* 86, 032710 (2012).
- [21] A.B. Voitkiv, B. Najjari, J. Ullrich, *J. Phys. B* 36, 2591 (2003).
- [22] M. Foster, D.H. Madison, J.L. Peacher, and J. Ullrich, *J. Phys. B* 37, 3797 (2004).
- [23] K.N. Egodapitiya, S. Sharma, A. Hasan, A.C. Laforge, D.H. Madison, R. Moshhammer, and M. Schulz, *Phys. Rev. Lett.* 106, 153202 (2011).
- [24] X. Wang, K. Schneider, A. LaForge, A. Kelkar, M. Grieser, R. Moshhammer, J. Ullrich, M. Schulz, and D. Fischer, *J. Phys. B* 45, 211001 (2012).
- [25] S. Sharma, A. Hasan, K.N. Egodapitiya, T.P. Arthanayaka, and M. Schulz, *Phys. Rev. A* 86, 022706 (2012).
- [26] G.B. Crooks and M.E. Rudd, *Phys. Rev. Lett.* 25, 1599 (1970).
- [27] L. Sarkadi, J. Pálkás, A. Kövér, D. Berényi, and T. Vajnai, *Phys. Rev. Lett.* 62, 527 (1989).
- [28] D.H. Lee, P. Richard, T.J.M. Zouros, J.M. Sanders, J.L. Shinpaugh, and H. Hidmi, *Phys. Rev. A* 41, 4816 (1990).
- [29] T. Vajnai, A.D. Gaus, J.A. Brand, W. Htwe, D.H. Madison, R.E. Olson, J.L. Peacher, and M. Schulz, *Phys. Rev. Lett.* 74, 3588 (1995).
- [30] A. Salin, *J. Phys. B* 2, 631 (1969).
- [31] A.D. Gaus, W. Htwe, J.A. Brand, T.J. Gay, and M. Schulz, *Rev. Sci. Instrum.* 65, 3739 (1994).
- [32] J.T. Park in “Collision Spectroscopy” (R.G. Cooks, ed.), p. 19, Plenum Publishing Co., New York (1978).
- [33] M. F. Ciappina, C. A. Tachino, R. D. Rivarola, S. Sharma and M. Schulz, *J. Phys. B* 48, 115204 (2015).
- [34] U. Chowdhury, M. Schulz, and D.H. Madison, *Phys. Rev. A* 83, 032712 (2011).
- [35] S. Sharma, T.P. Arthanayaka, A. Hasan, B.R. Lamichhane, J. Remolina, A. Smith, and M. Schulz, *Phys. Rev. A* 89, 052703 (2014).
- [36] M.B. Shah, C. McGrath, C. Illescas, B. Pons, A. Riera, H. Luna, D.S.F. Crothers, S.F.C. O’Rourke, and H.B. Gilbody, *Phys. Rev. A* 67, 010704 (2003).

#### IV. Fully differential study of wave packet scattering in ionization of Helium by proton impact

T. Arthanayaka<sup>1</sup>, B.R. Lamichhane<sup>1</sup>, A. Hasan<sup>1,2</sup>, S. Gurung<sup>1</sup>, J. Remolina<sup>1</sup>, S. Borbély<sup>3</sup>,  
F. Járαι-Szabó<sup>3</sup>, L. Nagy<sup>3</sup>, and M. Schulz<sup>1</sup>

<sup>1</sup>*Dept. of Physics and LAMOR, Missouri University of Science & Technology, Rolla, MO  
65409*

<sup>2</sup>*Dept. of Physics, UAE University, P.O. Box 15551, Al Ain, Abu Dhabi, UAE*

<sup>3</sup>*Faculty of Physics, Babes-Bolyai University, Kogalniceanu St. 1, 400084 Cluj, Romania*

#### Abstract

We present a fully differential study of projectile coherence effects in ionization in  $p + \text{He}$  collisions. The experimental data are qualitatively reproduced by a non-perturbative *ab initio* time-dependent model, which treats the projectile coherence properties in terms of a wave packet. A comparison between first- and higher-order treatments shows that the observed interference structures are primarily due to a coherent superposition of different impact parameters leading to the same scattering angle. Higher-order contributions have a significant effect on the interference term.

#### Introduction

It is well established that matter waves can show similar interference effects as light [e.g. 1-3]. Furthermore, as in classical optics, one requirement for observable interference phenomena is that the incoming waves must be coherent over the dimension of the diffracting object [e.g. 4-6]. However, in theoretical calculations of scattering cross



sections not much attention was paid to the coherence properties of the projectiles. Rather, the incoming projectiles were usually assumed to be fully coherent. For electron impact, this is in most cases a justified assumption because there the coherence length tends to be very large due to the large de Broglie wavelengths of electrons even at large energies. For ion impact, on the other hand, for which the coherence lengths tend to be orders of magnitude smaller, multiple differential measurements of cross sections as a function of projectile parameters were very rare until about 10 to 15 years ago [7,8]. Less differential measurements, especially those integrating over projectile parameters, are not very sensitive to the projectile coherence properties so that here the assumption of a fully coherent beam may have not been critical either.

With the advent of cold target recoil-ion momentum spectroscopy (COLTRIMS) [9,10] fully differential measurements on ionization by ion impact became feasible [e.g. 11-13, for a review see 14]. These studies revealed surprising discrepancies between experiment and theory which resisted an explanation for about a decade. Then, a few years ago, experimental data were reported which suggested that double differential ionization cross sections as a function of projectile energy loss and scattering angle in  $p + H_2$  collisions were significantly affected by the projectile coherence properties [5]. More specifically, interference structures were observed when projectiles with a large transverse coherence length  $\Delta x$  were prepared, but they were absent for a small  $\Delta x$ . More recent experimental data suggest that the discrepancies in the fully differential cross sections mentioned above may be due to an unrealistic description of the projectile coherence properties in theory [15,16]. Another fully differential study yielded good agreement between experiment and theory for relatively large  $\Delta x$  (compared to the relatively small impact parameters mostly

contributing to ionization for fast ion impact) and is thus consistent with this interpretation, although no conclusive evidence neither supporting nor dismissing it was reported [17].

Further support for an important role of coherence effects, initially observed in double differential cross sections for  $p + H_2$  collisions, was later obtained from measurements of fully differential cross sections (FDCS) for the same collision system [18,19]. These data were interpreted in terms of two different types of interference being present in the FDCS for coherent projectiles, which were dubbed molecular two-center and single-center interference, respectively [19]. The former is due to indistinguishable diffraction of the projectile from the two atomic centers in the molecule. The latter was initially interpreted as interference between first- and higher-order transition amplitudes; however, here we will show that this interpretation may have to be modified. The simultaneous presence of both types of interference makes the analysis of coherence effects and of the interference term difficult.

Another limitation in advancing our understanding of such effects from the existing data is that only very little theoretical work has been done in which the projectile coherence properties are incorporated in terms of a wave packet approach [20]. Results of calculations considering the projectile coherence properties by *ad hoc* approaches [18,19,21] provide encouraging qualitative support of the interpretation of experimental data, but they do not offer ultimate evidence. Indeed, this interpretation did not go completely unchallenged. Feagin and Hargreaves [22] argued that the differences between the cross sections for coherent and incoherent projectiles were merely due to differences in the beam divergence. However, Sharma et al. [23] demonstrated that there was no significant difference in the beam divergence for the measurement of the coherent and

incoherent cross sections. On the other hand, Walters and Whelan [24], using a sophisticated non-perturbative approach with a two-center basis, found significant coherence effects in the double differential ionization cross sections for  $p + H$  collisions, which resembled experimental observations for  $p + H_2$  collisions. But there, too, the coherence properties were not treated by describing the projectile by a wave packet. Only very recently a theoretical study treating the projectile by a wave packet was reported [20]. The authors of that work concluded that indeed the experimental observations reported in [5] are due to the projectile coherence properties and are not merely due to a beam divergence effect.

In this Letter, we present a fully differential study of coherence effects for ionization of an atomic target. Since here molecular two-center interference is obviously absent, single-center interference could be analyzed unambiguously. The experimental data are compared to a time-dependent *ab initio* calculation, in which the projectile is described in terms of a wave packet and in which the initial width of the wave packet reflects the transverse coherence length of the projectiles. Qualitatively good agreement between experiment and theory is found.

## Experiment

The experiment was performed at *Missouri S&T*. A 75 keV proton beam was collimated by a pair of slits with a width of 150  $\mu\text{m}$ . The slit collimating in the vertical (y) direction was kept at a fixed distance of 50 cm from the target, while in the horizontal (x) direction two different distances of  $L_1 = 50$  cm and  $L_2 = 6.5$  cm were used. These slit geometries correspond to transverse projectile coherence lengths  $\Delta x$  of about 3.5 and 1.0 a.u.,

respectively (for more details see [18]). It should be noted that for the low-energy protons studied here typical impact parameters are significantly larger than for the much faster protons studied in [17]. As a result, although  $\Delta x$  for the small slit distance is similar to the one realized in [17], relative to the effective dimension of the diffracting object (i.e. the impact parameters)  $\Delta x$  is much smaller. Projectiles which did not charge-exchange in the collision were selected by a switching magnet, decelerated to 5 keV, and energy-analyzed by an electrostatic parallel plate analyzer [25]. The analyzer slits were narrow in the  $y$ -direction (75  $\mu\text{m}$ ), but long in the  $x$ -direction (2.5 cm). Protons which suffered an energy loss of  $\varepsilon = 30$  eV passed the entrance and exit slits and were detected by a two-dimensional position-sensitive channel-plate detector. The position information in the  $x$ -direction provided the  $x$ -component of the momentum transfer  $\mathbf{q}$  from the projectile to the target while the  $y$ -component is fixed at zero (within the experimental resolution) due to the narrow analyzer slit width. The  $z$ -component is related to the energy loss by  $q_z = \varepsilon/v$ , where  $v$  is the projectile velocity.

A very cold He beam ( $T \approx 1\text{-}2$  K) was produced by a supersonic jet expanding in the  $y$ -direction. In that direction the He beam is cooled by adiabatic expansion due to the large pressure gradient between the gas reservoir and the surrounding chamber. Before entering the collision region the He atoms are well collimated by a conically shaped skimmer minimizing scattering from the skimmer itself. This collimation results in a target temperature in the  $xz$ -plane which is nearly an order of magnitude lower than in the  $y$ -direction. As a result, the corresponding momentum spread in the direction of the scattering ( $x$ -direction) does not make a significant contribution to the coherence properties of the collision.

The recoiling target ions were extracted by a weak electric field ( $E = 8 \text{ V/cm}$ ) pointing in the x-direction and also detected by a two-dimensional position-sensitive channel-plate detector. From the position information the recoil-ion momentum components in the y- and z-direction (defined by the initial projectile beam axis) are extracted. The projectile and recoil-ion detectors are set in coincidence. Since the projectile time of flight is fixed the coincidence time directly reflects the recoil-ion time of flight so that it provides the recoil-ion momentum in the x-direction. The electron momentum is deduced from momentum conservation by  $\mathbf{p}_{\text{el}} = \mathbf{q} - \mathbf{p}_{\text{rec}}$ .

Our theoretical approach to account for the projectile coherence properties in the description of the ionization process builds on the method reported earlier in [21]. There, as a first step, we calculated an impact parameter ( $\mathbf{b}$ ) dependent transition amplitude  $a(\mathbf{b}, \mathbf{p}_{\text{el}})$ , where  $\mathbf{p}_{\text{el}}$  is the ejected electron momentum. In the incoherent case we assigned to each impact parameter a certain projectile scattering angle (and thus perpendicular momentum transfer  $\mathbf{q}_{\perp}$ ) on the basis of classical scattering. In the coherent case we calculated the scattering amplitude  $R(\mathbf{q}_{\perp}, \mathbf{p}_{\text{el}})$  by an inverse Fourier transform (Eq. 4 of [21]).

Here, we complete our model by describing the projectile as a wave packet with finite coherence length  $\Delta b$ . In the previously mentioned inverse Fourier transform the transition amplitude is multiplied by a Gaussian profile centered on the impact parameter  $b_0$  assigned to the momentum transfer  $\mathbf{q}_{\perp}$  for the incoherent case

$$R(\mathbf{q}_{\perp}, \mathbf{p}_{\text{el}}) = \frac{c}{2\pi} \int d\mathbf{b} a(\mathbf{b}, \mathbf{p}_{\text{el}}) e^{i\mathbf{b} \cdot \mathbf{q}_{\perp}} b^{2i \frac{Z_{\text{p}} Z_{\text{t}}}{v}} e^{-\frac{(b_0 - b)^2}{2\Delta b^2}} \quad (1)$$

Here,  $C$  is a normalization constant and  $b^{2i\frac{Z_p Z_t}{v}}$  is an eikonal phase accounting for the internuclear interaction,  $Z_p$  and  $Z_t$  being the charges of the projectile and the target nucleus, respectively.

It should be emphasized that the projectile coherence properties are actually determined by the intrinsic momentum spread, i.e. by the width of the projectile wave packet in momentum space. In the transverse direction, this momentum spread is given by the local collimation angle that the slit subtends relative to the target location [e.g. 4]. Although the slit width is of macroscopic dimension, the momentum spread defined by the local collimation angle is of microscopic (atomic) magnitude, i.e. the macroscopic slit width does not rule out an influence on the microscopic coherence length. Furthermore, it should be noted that, although the width of the projectile wave packet in position space increases due to dispersion, the momentum spread remains fixed in free propagation so that dispersion has no effect on the coherence properties. In our model dispersion is neglected because the wave packet is time-independent. In this approximation the transverse coherence length is determined by the width of the wave packet in position space, which in turn is related to the wave packet in momentum space by a Fourier transform.

The amplitude  $a(\mathbf{b}, \mathbf{p}_{e1})$  is calculated in two ways: applying a perturbation and an *ab initio* model. In the latter, the two-electron time-dependent Schrödinger equation is solved numerically [26], and from the obtained fully-correlated electronic wave function the ionization probability amplitudes are extracted by projecting onto single continuum eigenstates. Since these single continuum states are calculated in the field of the residual ion, the electron population captured by the projectile is also counted as ionization. This

contamination is significant in the vicinity of the projectile velocity (forward ejection angles), but its influence becomes negligible for larger angles.

## Results and Discussions

Before we discuss the FDCS we first analyze the ratio  $R$  between the double differential cross sections DDCS measured for the slit distances  $L_1$  and  $L_2$  for  $\varepsilon = 30$  eV as a function of either the projectile scattering angle  $\theta_p$  or  $p_{\text{recx}}$ . Since these slit distances correspond to large and small transverse coherence lengths, we refer to these DDCS as the coherent and incoherent cross sections, respectively. These  $R$ , which reflect the interference term [18,19], are plotted as a function of  $\theta_p$  (closed symbols, lower scale) and  $p_{\text{recx}}$  (open symbols, upper scale) of figure 1. The phase angle in the two-center interference term depends on the recoil-ion momentum [27], while for single-center interference it depends on the transverse component of  $\mathbf{q}$  [24]. We would therefore expect structures in  $R(\theta_p)$ , but a flat dependence in  $R(p_{\text{recx}})$ , which is exactly what is observed in figure 1.

For the presentation of the FDCS we use a coordinate system in which the positive x-direction is defined by the transverse component of  $\mathbf{q}$  and the z-direction by the initial projectile beam axis, i.e.  $q_x \geq 0$  and  $q_y = 0$  for all events. The FDCS are analyzed for fixed  $\varepsilon = 30$  eV and various fixed values of  $p_{\text{recx}}$  and presented as a function of the polar and azimuthal electron ejection angles  $\theta_{\text{el}}$  and  $\phi_{\text{el}}$ . Here,  $\theta_{\text{el}}$  is measured relative to the z-axis and  $\phi_{\text{el}}$  is, somewhat unconventionally, the angle between the positive y-axis and the projection of  $\mathbf{p}_{\text{el}}$  onto the xy-plane. Therefore,  $\phi_{\text{el}} = 90^\circ$  corresponds to the direction of the transverse component of  $\mathbf{q}$ . It should be noted that in this representation of the FDCS each

combination of  $\theta_{el}$  and  $\phi_{el}$  unambiguously correspond to a well-defined value of  $q_x$  according to  $q_x = p_{el} \sin\theta_{el} \sin\phi_{el} + p_{recx}$ .

In figure 2 the FDCS measured with a coherent (panel a) and incoherent (panel b) projectile beam are plotted for  $p_{recx} = 1.25$  a.u. as a function of  $\theta_{el}$  and  $\phi_{el}$ . In both cases a maximum is observed around  $\theta_{el} = 45^\circ$  and  $\phi_{el} = 270^\circ$ . If the FDCS are presented for fixed  $q$ , the so-called binary peak, occurring at  $\phi_{el} = 90^\circ$  and  $\theta_{el}$  between  $0^\circ$  and  $90^\circ$ , is usually the dominant structure. The reason that in our presentation of the FDCS (i.e. for fixed  $p_{recx}$ ) the binary peak is very weak (if present at all) is that the angle-dependent  $q$  maximizes for  $\phi_{el} = 90^\circ$ . The cross sections, on the other hand, are known to steeply decrease with increasing  $q$ .

Significant differences between the coherent and incoherent data are quite apparent. Most notably, the latter are more spread out than the former in both the  $\theta_{el}$  - and  $\phi_{el}$  - dependencies. Panels c) and d) show the coherent and incoherent FDCS calculated with the perturbative model and panels e) and f) those calculated with the *ab initio* model. The perturbative calculation does not even reproduce the experimental data qualitatively, as expected for the relatively large perturbation parameter of  $\eta = Z_p/v = 0.6$ . Much improved agreement is achieved with the *ab initio* model. Nevertheless, there are still some discrepancies in the peak position, which is shifted relative to the measured FDCS in the forward direction. This is probably due to a large loss of flux to the capture channel, which is considered as ionization in the calculation, especially at small  $\theta_{el}$  [28,29]. On the other hand, the calculation quite well reproduces the spreading of the incoherent relative to the coherent experimental data in the  $\theta_{el}$  - and  $\phi_{el}$  - dependencies of the FDCS.



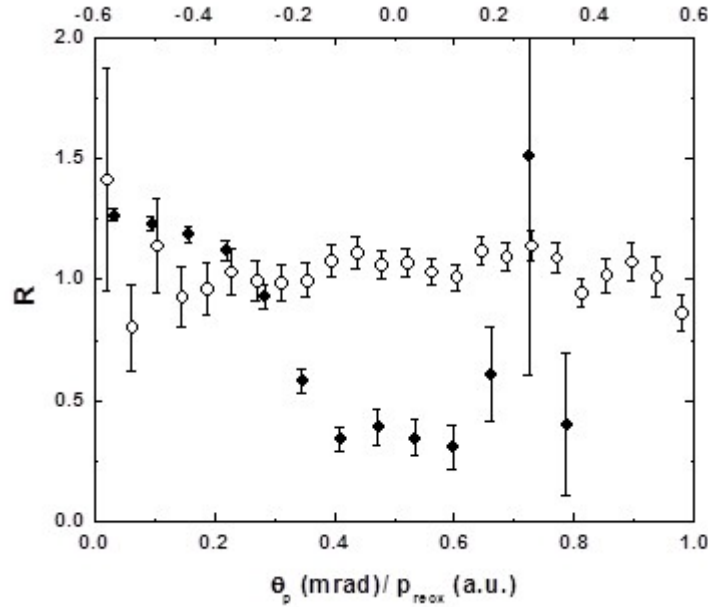


Figure 1. Ratios between double differential cross sections measured for coherent and incoherent projectile as a function of scattering angle (closed symbols, lower scale) and the x-component of the recoil-ion momentum (open symbols, upper scale).

In order to analyze coherence effects and the interference term in more detail, we show in figure 3 the ratio  $R$  between the coherent and incoherent FDCS (which represents the interference term) as a function of  $\phi_{el}$  for  $p_{reco} = 0.2$  a.u. and  $\theta_{el} = 25^\circ$  (panel a),  $p_{reco} = 0.7$  a.u. and  $\theta_{el} = 45^\circ$  (panel b),  $p_{reco} = 0.7$  a.u. and  $\theta_{el} = 65^\circ$  (panel c), and  $p_{reco} = 1.25$  a.u. and  $\theta_{el} = 65^\circ$  (panel d). The shape of  $R(\phi_{el})$  varies significantly with the kinematic parameters. At small  $p_{reco}$  and  $\theta_{el}$   $R$  is essentially constant and no clear coherence effects are discerned. However, with increasing  $p_{reco}$  and  $\theta_{el}$  an increasingly pronounced structure is observed which changes in shape with both  $p_{reco}$  and  $\theta_{el}$ . In all cases, except for  $p_{reco} = 0.2$  a.u. and  $\theta_{el} = 25^\circ$ , a pronounced minimum is found at  $\phi_{el} = 90^\circ$ . But at  $\phi_{el} = 270^\circ$  the shape ranges from a shallow minimum for  $p_{reco} = 0.7$  a.u. and  $\theta_{el} = 45^\circ$  to a deep minimum for  $p_{reco} = 0.7$  a.u. and  $\theta_{el} = 65^\circ$ , to a maximum for  $p_{reco} = 1.25$  a.u. and  $\theta_{el} = 65^\circ$ .

The dashed and solid curves in figure 3 show the results of our perturbative and *ab initio* calculations, respectively. Both models reproduce the basic features seen in the experimental data, including the transition from a minimum to a maximum at  $\phi_{el} = 270^\circ$  going from  $p_{recx} = 0.7$  to 1.25 a.u., although overall the *ab initio* results are in somewhat better agreement with the data. One striking feature in the data, which is qualitatively well reproduced by the *ab initio* calculation, is that the minimum in R at  $90^\circ$  for the largest recoil momentum is particularly pronounced. This reflects that essentially no counts were detected for the coherent case, while the incoherent signal was quite strong.

Considering the major discrepancies between the measured FDCS and the perturbative model, the agreement in the ratios is remarkably good. Since this model does not account for higher-order contributions in the projectile-electron interaction (to which we refer in the following as post-collision interaction or PCI), this suggests that the interference term is much less sensitive to such contributions than the FDCS. This assumption is further supported by the similarity of the perturbative results to the *ab initio* calculations, which fully accounts for PCI.

To further test the effect of higher-order contributions on the interference term we have computed R using the perturbative model with the eikonal phase, describing the nucleus-nucleus interaction, removed. These calculations, which are shown as dotted curves in figure 3, represent a pure first-order treatment. Nevertheless, pronounced structures are still observable. This shows that our original interpretation of single-center interference, as being due to a coherent superposition of first- and higher-order transition amplitudes [19], has to be modified. Rather, based on the present calculations, we conclude that the interference is due to a coherent superposition of different impact parameters

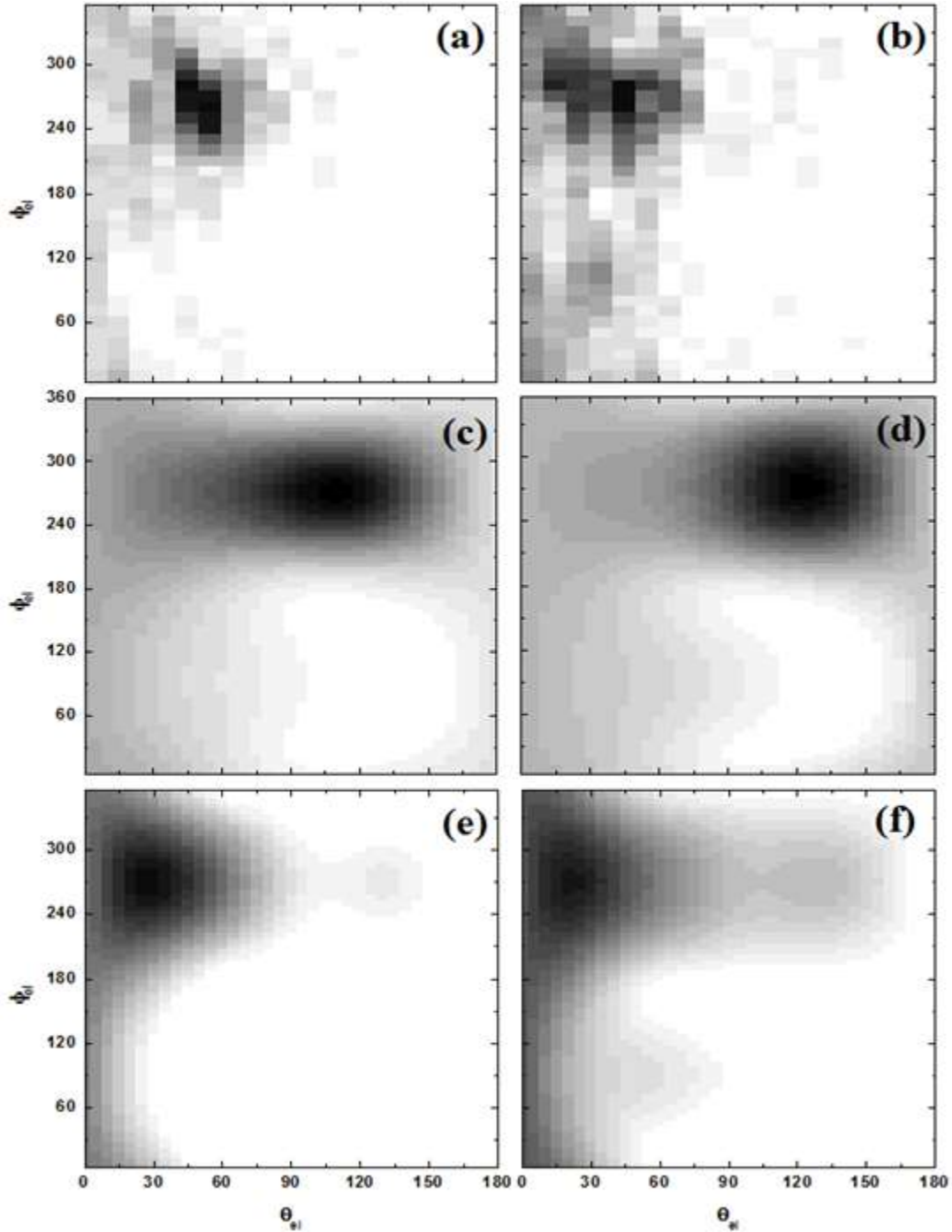


Figure 2. Fully differential cross sections for fixed projectile energy loss ( $\varepsilon = 30$  eV) and fixed x-component of the recoil-ion momentum ( $p_{\text{reco}} = 1.25$  a.u.) as a function of the azimuthal and polar electron emission angles. The left panels represent coherent and the right panels incoherent cross sections. Panels a) and b), experiment; panels c) and d) perturbative model, panels e) and f) *ab initio* model.

resulting in the same scattering angle, independent of the importance of higher-order contributions. Even in a coherent first-order treatment such interference is present through the Fourier transform relating the scattering-angle dependent to the impact parameter

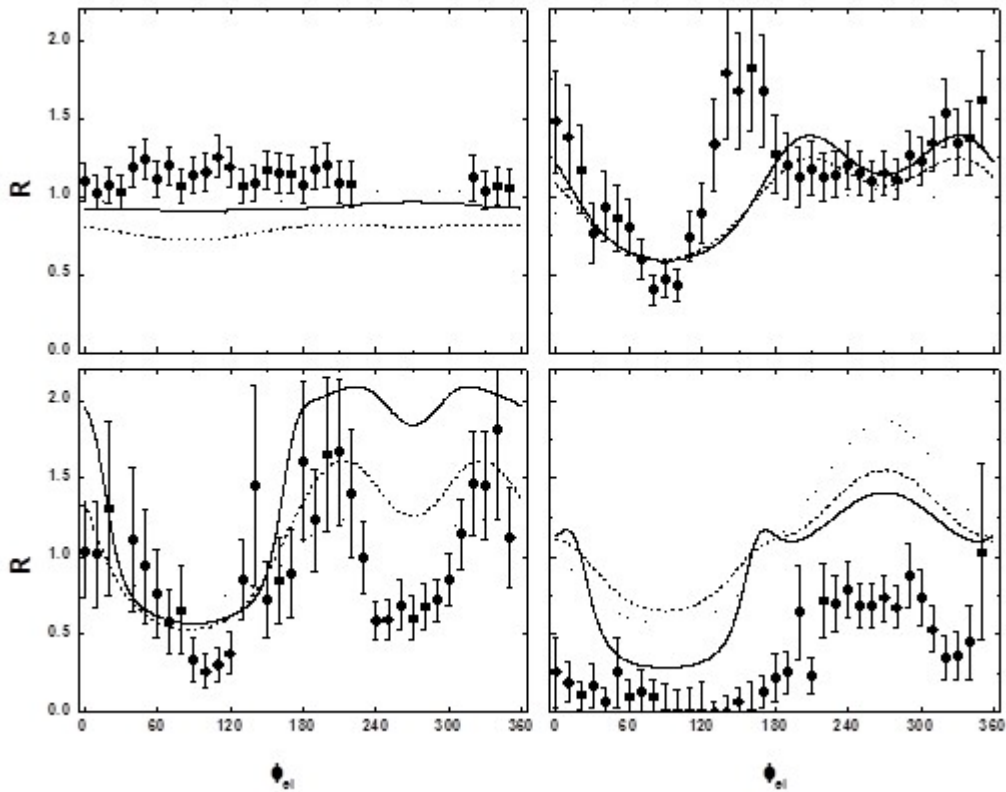


Figure 3. Ratios between FDCS for coherent and incoherent beams  $p_{\text{recx}} = 0.2$  a.u. and  $\theta_{\text{el}} = 25^\circ$  (panel a),  $p_{\text{recx}} = 0.7$  a.u. and  $\theta_{\text{el}} = 45^\circ$  (panel b),  $p_{\text{recx}} = 0.7$  a.u. and  $\theta_{\text{el}} = 65^\circ$  (panel c), and  $p_{\text{recx}} = 1.25$  a.u. and  $\theta_{\text{el}} = 65^\circ$  (panel d) as a function  $\phi_{\text{el}}$ . Dotted curves, perturbative model without eikonal phase; dashed curves, perturbative model with eikonal phase; solid curves, *ab initio* model.

dependent transition amplitude. Nevertheless, the differences between the various calculations show that higher-order effects, both in the nucleus-nucleus interaction (not included in the perturbative model without eikonal phase) and in the projectile – electron

interaction (only accounted for in the *ab initio* model) play an important role in the interference term.

## Conclusions

In summary, we have performed a joint experimental and theoretical fully differential study of wave packet scattering in ionization in  $p + \text{He}$  collisions. The experimentally observed projectile coherence effects are qualitatively reproduced by our calculations. Over the last five years numerous experimental studies supporting an important role of projectile coherence effects were reported. With the present work this interpretation of the data is now backed by a theoretical analysis which goes well beyond an *ad hoc* approach and which describes the projectile by a wave packet. For collision systems involving intermediate energies, like the one studied here, we therefore believe that the existence of projectile coherence effects can now be regarded as established beyond reasonable doubt. In contrast, for fast ion impact a confirmation of the role of coherence effects on the FDCS requires further experimental and theoretical work.

The comparison between first-order and high-order treatments demonstrates that single-center interference is primarily due to a coherent superposition of different impact parameters leading to the same scattering angle, but higher-order contributions nevertheless play an important role in the interference term. To achieve improved quantitative agreement between experiment and theory it seems important to extend the *ab initio* model to a two-center basis set so that the capture channel is adequately accounted for.

## Acknowledgements

This work was supported by the National Science Foundation under grant no. PHY-1401586, a grant of the Romanian National Authority for Scientific Research project number PN-II-ID-PCE-2011-3-0192 and the Hungarian OTKA K103917 project.

## References

- [1] C. Davisson, *Journal of the Franklin Institute* 205, 597 (1928).
- [2] N. Stolterfoht, B. Sulik, V. Hoffmann, B. Skogvall, J. Y. Chesnel, J. Ragnama, F. Frémont, D. Hennecart, A. Cassimi, X. Husson, A. L. Landers, J. Tanis, M. E. Galassi, and R. D. Rivarola, *Phys. Rev. Lett.* 87, 23201 (2001).
- [3] L.P.H. Schmidt, S. Schössler, F. Afaneh, M. Schöffler, K. E. Stiebing, H. Schmidt-Böcking, and R. Dörner, *Phys. Rev. Lett.* 101, 173202 (2008).
- [4] A.D. Cronin, J. Schmiedmayer, D.E. Pritchard, *Reviews of Modern Physics* **81**, 1051 (2009).
- [5] K. N. Egodapitiya, S. Sharma, A. Hasan, A. C. Laforge, D. H. Madison, R. Moshhammer, and M. Schulz, *Phys. Rev. Lett.* 106, 153202 (2011).
- [6] C. Keller, J. Schmiedmayer, and A. Zeilinger, *Opt. Comm.* 179, 129 (2000).
- [7] T. Vajnai, A.D. Gaus, J.A. Brand, W. Htwe, D.H. Madison, R.E. Olson, J.L. Peacher, and M. Schulz, *Phys. Rev. Lett.* 74, 3588 (1995).
- [8] R. Dörner, H. Khemliche, M.H. Prior, C.L. Cocke, J.A. Gary, R.E. Olson, V. Mergel, J. Ullrich, and H. Schmidt-Böcking, *Phys. Rev. Lett.* 77, 4520 (1996).
- [9] R. Dörner, V. Mergel, O. Jagutzski, L. Spielberger, J. Ullrich, R. Moshhammer, and H. Schmidt-Böcking, *Phys. Rep.* 330, 95 (2000).
- [10] J. Ullrich, R. Moshhammer, A. Dorn, R. Dörner, L. Schmidt, and H. Schmidt-Böcking, *Rep. Prog. Phys.* 66, 1463 (2003).
- [11] M. Schulz, R. Moshhammer, D. Fischer, H. Kollmus, D.H. Madison, S. Jones, and J. Ullrich, *Nature* 422, 48 (2003).

- [12] N.V. Maydanyuk, A. Hasan, M. Foster, B. Tooke, E. Nanni, D.H. Madison, and M. Schulz, *Phys. Rev. Lett.* 94, 243201 (2005).
- [13] M. Schulz, B. Najjari, A.B. Voitkiv, K. Schneider, X. Wang, A.C. Laforge, R. Hubele, J. Goullon, N. Ferreira, A. Kelkar, M. Grieser, R. Moshhammer, J. Ullrich, and D. Fischer, *Phys. Rev. A* 88, 022704 (2013).
- [14] M. Schulz and D.H. Madison, *International Journal of Modern Physics A* 21, 3649 (2006).
- [15] X. Wang, K. Schneider, A. LaForge, A. Kelkar, M. Grieser, R. Moshhammer, J. Ullrich, M. Schulz, and D. Fischer, *J. Phys. B* 45, 211001 (2012).
- [16] K. Schneider, M. Schulz, X. Wang, A. Kelkar, M. Grieser, C. Krantz, J. Ullrich, R. Moshhammer, and D. Fischer, *Phys. Rev. Lett.* 110, 113201 (2013).
- [17] H. Gassert et al., *Phys. Rev. Lett.* 116, 073201 (2016).
- [18] S. Sharma, T.P. Arthanayaka, A. Hasan, B.R. Lamichhane, J. Remolina, A. Smith, and M. Schulz, *Phys. Rev. A* 90, 052710 (2014).
- [19] T.P. Arthanayaka, S. Sharma, B.R. Lamichhane, A. Hasan, J. Remolina, S. Gurung, and M. Schulz, *J. Phys. B* 48, 071001 (2015).
- [20] L. Sarkadi, I. Fabre, F. Navarrete, and R.O. Barrachina, *Phys. Rev. A* 93, 032702 (2016).
- [21] F. Jarai-Szabo and L. Nagy, *Eur. Phys. J. D* 69, 4 (2015).
- [22] J.M. Feagin and L. Hargreaves, *Phys. Rev. A* 88, 032705 (2013).
- [23] S. Sharma, T.P. Arthanayaka, A. Hasan, B.R. Lamichhane, J. Remolina, A. Smith, and M. Schulz, *Phys. Rev. A* 89, 052703 (2014).
- [24] H.R.J. Walters and C.T. Whelan, *Phys. Rev. A* 92, 062712 (2015).
- [25] A.D. Gaus, W. Htwe, J.A. Brand, T.J. Gay, and M. Schulz, *Rev. Sci. Instrum.* 65, 3739 (1994).
- [26] S. Borbély, J. Feist, K. Tókési, S. Nagele, L. Nagy and J. Burgdörfer, *Phys. Rev. A* 90 052706 (2014).
- [27] S.E. Corchs, R.D. Rivarola, J.H. McGuire, and Y.D. Wang, *Phys. Scr.* 50, 469 (1994).

- [28] A. Hasan, S. Sharma, T.P. Arthanayaka, B.R. Lamichhane, J. Remolina, S. Akula, D.H. Madison, and M. Schulz, *J. Phys. B* 47, 215201 (2014).
- [29] A. Hasan, T. Arthanayaka, B.R. Lamichhane, S. Sharma, S. Gurung, J. Remolina, S. Akula, D.H. Madison, M.F. Ciappina, R.D. Rivarola, and M. Schulz, *J. Phys. B* 49, Letter, 04LT01 (2016).



## SECTION

### 2. CONCLUSION

It is well established that Young type interference structures can be observed in ionization of molecular  $H_2$ . This interference is mainly due to indistinguishable scattering from the two atomic centers of the molecule. Earlier Egodapitiya et al [27] tested this idea by performing an experiment on single ionization of  $H_2$  by proton impact. They have observed, that the measured double differential cross sections (DDCS) are very sensitive to the coherence length of the projectile. By varying the geometry of the collimating slit, which was placed before the target, they controlled the projectile coherence length. That experiment thus qualitatively demonstrated the importance of the projectile coherence properties. Sharma et al [35] further support the role of coherence effects by performing fully differential cross sections (FDCS) measurements for the same collision system. There, two different types of interference structures were discussed, namely molecular two-center and single-center interference. However, the data were not sensitive enough to conclusively identify and distinguish between single- and two-center interference. This dissertation is comprised of four papers and there a series of experiments was performed to address such questions in more detail.

We have performed a kinematically complete experiment for ionization of  $H_2$  by 75 keV p impact for an energy loss of 57 eV, which corresponds to an electron energy of 41.4 eV. In the first journal article of my dissertation, the aim was to address the discrepancies of the phase angle dependence in the FDCS observed by Sharma et al [35] and to investigate single-center interference and two-center interference further. The data

were obtained for two transverse coherence lengths of 3.3 a.u. (coherent projectile) and 0.4 -1.0 a.u. (incoherent projectile) as discussed in the referred article. Relatively small, but significant differences between both data sets were observed as a function of the azimuthal electron ejection angle  $\varphi_{el}$  for fixed polar electron emission angle  $\theta_{el}$  and fixed  $q$ . A comparably strong interference structure, with a  $\mathbf{p}_{rec}$ -dependent phase angle, was experimentally observed. This was interpreted as two-center molecular interference. Furthermore, a pronounced interference structure was also observed if the data were plotted for fixed  $\theta_{el}$  and  $\mathbf{p}_{rec}$  as a function of  $\varphi_{el}$ . In this representation of the data any structure as a function of  $\varphi_{el}$  means that the phase angle depends on  $q$ . In the article, the importance of both single- and two-center interference was thus identified in ionization of  $H_2$  and both types of interference structures were separated by fixing the momentum transfer and the recoil momentum of the FDCS, respectively, separated both type of interference structures.

Earlier, Alexander et al [36] found that interference is suppressed at  $\varepsilon = 57$  eV, where the ejected electron speed is equal to the projectile speed. Since it is known, that for this velocity matching, the post-collision interaction (PCI) can play a very important role in effective cross sections. Alexander et al consider the possibility that the suppressed interference structure might be related to a loss of coherence caused by PCI. However, for two reasons this experiment was not sensitive enough to conclusively address this question. First, the experiment was not kinematically complete, therefore depth analysis of the collision dynamics is limited. Second, at the time it was not clear how to test coherence effects experimentally. In the first journal article of my dissertation, analysis of single- and two- center interference were presented. However, a possible connection between interference and PCI effects were not addressed in that work. In the second journal article,

the results of a kinematically complete experiment is presented and the data were analyzed under kinematic conditions either favoring or suppressing PCI. It has been demonstrated, that setting a condition on the longitudinal recoil-ion momentum is an effective method to separate PCI favoring or suppressing effects. Therefore, such a separation allowed to analyze the interference term under varying PCI conditions. For all kinematic settings less pronounced interference structures with a  $q$ -dependent phase angle were observed than at small energies  $\varepsilon = 30$  eV, independent of PCI settings. Furthermore, a less pronounced interference structure was observed for strong PCI compared to weak PCI. These observations shows that indeed PCI leads to a loss of coherence. However, this does mostly lead to a suppression of single-center interference, rather than two-center interference, as assumed by Alexander et al.

In the third journal article, the first experiment of FDCS for target ionization by ion impact, leading to ejected electrons with a speed equal to the projectile speed, is presented. The experimental results are compared with the molecular continuum distorted wave Eikonal initial state approximation (CDW-EIS MO) and the molecular three-body distorted wave Eikonal initial state (M3DW-EIS) models. Severe discrepancies were found between the measured and calculated FDCS. Most notably, when the FDCS are plotted as a function of the polar electron ejection angle  $\theta_{el}$  for energy loss and momentum transfer  $q$ , a very sharp and large peak structure is found at  $\theta_{el} = 0$  specially for small scattering angles in both calculations, which is to a large extend absent in the measured FDCS. Furthermore, for all  $q$  the height of the  $0^\circ$  peak in the calculations is much larger than the magnitude of the binary peak in the experimental FDCS. Our data suggest that the coupling between capture and ionization channel could be responsible for these discrepancies, which is not

accounted for in the calculations. For  $v_{el} \approx v_p$  (i.e.  $\varepsilon = 57$  eV and  $\theta_{el} = 0$ ) the capture probability could saturate leading to a strong depletion of the FDCS for ionization and this would explain the strong suppression of the  $0^\circ$  peak in the experimental data.

Earlier we interpreted single-center interference as interference between first- and higher-order transition amplitudes; however in the fourth journal article we showed that this interpretation may have to be modified. In the  $p + H_2$  collision system, presence of both types of interference makes the analysis of coherence effects and of the interference term difficult. In the fourth journal article, a fully differential study of projectile coherence effects on ionization cross sections in  $p + He$  collisions is presented. FDCS measurements for He target for coherent and incoherent beam allow to unambiguously identify the single-center interference. This is a comparative study between experiments and *ab initio* calculations, which incorporate the projectile coherent properties in terms of a wave packet approach.

A pronounced structure was observed, for the coherent to incoherent double differential cross sectional DDCS ratio ( $R$ ) as a function of projectile scattering angle  $\theta_p$  ( $q = f(\theta_p)$ ), which conforms the presence of single-center interference. On the other hand a flat dependence of  $R$  is observed as function of  $p_{recx}$ , as we expected for He. Furthermore, significant differences between coherent and incoherent FDCS data were observed, as we analyzed the data for single-center interference. There was much improved agreement between the data and *ab initio* model, compared to perturbative *ad hoc* approaches. The comparison between first-order and high-order treatments of *ab initio* model to data demonstrates that single-center interference is primarily due to a coherent superposition of

different impact parameters leading to the same scattering angle. Nevertheless we conclude that higher-order interactions also have a significant effect in the single-center interference term.

**BIBLIOGRAPHY**

- [1] M. Schulz, R. Moshhammer, D. Fischer, H. Kollmus, D. H. Madison, S. Jones, and J. Ullrich, *Nature* **422** 48 (2003).
- [2] M. Schulz and D. H. Madison, *Int. J. Mod. Phys. A* **21**, 3649 (2006).
- [3] T.N. Rescigno, M. Baertschy, W.A. Isaacs, and C.W. McCurdy, *Science* **286**, 2474 (1999).
- [4] A.C. Laforge, K.N. Egodapitiya, J.S. Alexander, A. Hasan, M.F. Ciappina, M.A. Khakoo, and M. Schulz, *Phys. Rev. Lett.* **103**, 053201 (2009).
- [5] R. Dörner, V. Mergel, R. Ali, U. Buck, C.L. Cocke, K. Froschauer, O. Jagutzki, S. Lencinas, W.E. Meyerhof, S. Nüttgens, R. E. Olson, H. Schmidt-Böcking, L. Spielberger, K. Tökesi, J. Ullrich, M. Unverzagt, and W. Wu, *Phys. Rev. Lett.* **72**, 3166 (1994).
- [6] J. Ullrich, R. Moshhammer, R Dörner, O. Jagutzki, V. Mergel, H. Schmidt-Böcking and L. Spielberger, *J. Phys. B* **30**, 2917 (1997).
- [7] R. Moshhammer, M. Unverzagt, W. Schmitt, J. Ullrich, and H. Schmidt-Böcking, *Nucl. Instrum. Methods Phys. Res. B* **108**, 425 (1996).
- [8] J. Ullrich, R. Moshhammer, R. Dörner, O. Jagutzki, V. Mergel, H. Schmidt-Böcking and L. Spielberger, *Rep. Prog. Phys.* **66** 1463 (2003).
- [9] J. T. Park, J. E. Aldag, and J. M. George, *Phys. Rev. Lett.* **34**, 1253 (1975).
- [10] J. T. Park, J. E. Aldag, J. M. George, J. L. Peacher, and J. H. McGuire, *Phys. Rev. A* **15**, 508 (1977).
- [11] H. Ehrhardt, K. Jung, G. Knoth, and P. Schlemmer, *Z. Phys. D, Z. Phys. D* **1**, 3 (1986).
- [12] I. Bray, *J. Phys. B* **33**, 581 (2000).
- [13] J. Colgan, M. S. Pindzola, *Phys. Rev. A* **74**, 012713 (2006).
- [14] H. Ehrhardt, M. Schulz, T. Tekaas, and K. Willmann, *Phys. Rev. Lett.* **22**, 89 (1969).
- [15] M. Schulz, M. F. Ciappina, T. Kirchner, D. Fischer, R. Moshhammer, and J. Ullrich, *Phys. Rev. A* **79**, 042708 (2009).
- [16] M. Schulz, *Phys. Scr.* **80**, 068101 (2009).

- [17] M. F. Ciappina, W. R. Cravero, M. Schulz, R. Moshhammer, and J. Ullrich, *Phys. Rev. A* **74**, 042702 (2006).
- [18] A. B. Voitkiv and B. Najjari, *Phys. Rev. A* **79**, 022709 (2009).
- [19] D. H. Madison, D. Fischer, M. Foster, M. Schulz, R. Moshhammer, S. Jones, and J. Ullrich, *Phys. Rev. Lett.* **91**, 253201 (2003).
- [20] D. Madison, M. Schulz, S. Jones, M. Foster, R. Moshhammer and J. Ullrich, *J. Phys. B* **35** 3297 (2002).
- [21] R. E. Olson and J. Fiol, *Phys. Rev. Lett.* **95**, 263203 (2005).
- [22] J. Fiol, S. Otranto, and R. E. Olson, *J. Phys. B* **39**, L285 (2006).
- [23] M. Dürr, B. Najjari, M. Schulz, A. Dorn, R. Moshhammer, A. B. Voitkiv, and J. Ullrich, *Phys. Rev. A*, **75**, 062708 (2007).
- [24] M. Schulz, M. Dürr, B. Najjari, R. Moshhammer, and J. Ullrich, *Phys. Rev. A* **76**, 032712 (2007).
- [25] I. B. Abdurakhmanov, I. Bray, D. V. Fursa, A. S. Kadyrov, and A. T. Stelbovics, *Phys. Rev. A* **86**, 034701 (2012).
- [26] M. S. Pindzola and F. Robicheaux, *Phys. Rev. A* **82**, 042719 (2010).
- [27] K. N. Egodapitiya, S. Sharma, A. Hasan, A. C. Laforge, D. H. Madison, R. Moshhammer, and M. Schulz, *Phys. Rev. Lett.* **106**, 153202 (2011).
- [28] T. F. Tuan and E. Gerjuoy, *Phys. Rev.* **117**, 756 (1960).
- [29] H. D. Cohen and U. Fano, *Phys. Rev.* **150**, 30 (1966).
- [30] L. Ph. H. Schmidt, S. Schössler, F. Afaneh, M. Schöffler, K.E. Stiebing, H. Schmidt-Böcking, and R. Dörner, *Phys. Rev. A* **101**, 173202 (2008).
- [31] S. F. Zhang, D. Fischer, M. Schulz, A. B. Voitkiv, A. Senftleben, A. Dorn, J. Ullrich, X. Ma, and R. Moshhammer, *Phys. Rev. Lett.* **112**, 023201 (2014).
- [32] C. Keller, J. Schmiedmayer, and A. Zeilinger, *Optics Communications* **179**, 129 (2000).
- [33] X. Wang, K. Schneider, A. LaForge, A. Kelkar, M. Grieser, R. Moshhammer, J. Ullrich, M. Schulz and D Fischer, *J. Phys. B* **45**, 211001 (2012).

- [34] H. Gassert, O. Chuluunbaatar, M. Waitz, F. Trinter, H.-K. Kim, T. Bauer, A. Laucke, Ch. Müller, J. Voigtsberger, M. Weller, J. Rist, M. Pitzer, S. Zeller, T. Jahnke, L. Ph. H. Schmidt, J. B. Williams, S. A. Zaytsev, A. A. Bulychev, K. A. Kouzakov, H. Schmidt-Böcking, R. Dörner, Yu. V. Popov, and M. S. Schöffler, *Phys. Rev. Lett.* **116**, 073201 (2016).
- [35] S. Sharma, T.P. Arthanayaka, A. Hasan, B.R. Lamichhane, J. Remolina, A. Smith, and M. Schulz, *Phys. Rev. A* **90**, 052710 (2014).
- [36] J. S. Alexander, A. C. Laforge, A. Hasan, Z. S. Machavariani, M. F. Ciappina, R. D. Rivarola, D. H. Madison, and M. Schulz, *Phys. Rev. A* **78**, 060701(R) (2009).
- [37] M. Schulz, B. Najjari, A. B. Voitkiv, K. Schneider, X. Wang, A. C. Laforge, R. Hubele, J. Goullon, N. Ferreira, A. Kelkar, M. Grieser, R. Moshhammer, J. Ullrich, and D. Fischer, *Phys. Rev. A* **88**, 022704 (2013).



## VITA

Thusitha Priyantha Arthanayaka was born in Sandalankawa, North Western Province, Sri Lanka. After graduating from Sandalankawa National School in 2002, Thusitha went to University of Peradeniya, Sri Lanka. In May 2007, he graduated from faculty of science with Bachelor of Science (special) in physics. After graduation, he worked as a Teaching Assistant in the same faculty nearly more than a year. In August 2010, Thusitha enrolled at Missouri University of Science and Technology (Missouri S&T) where he obtained a MS (December 2014). In July 2016, he received his PhD in Physics from Missouri S&T, Rolla, Missouri, USA.

While at Missouri S&T, Thusitha has contributed for 8 publications (3 Phys. Rev. and 5 J. Phys B; one featured as an invited “LabTalk” presentation and other featured as video abstract) and 4 conference abstracts related to atomic collision experiments. Additionally, as a recognition of the research he had a chance to deliver an invited talk at APS 68th Annual GEC, Honolulu, HI, Oct 2015.

Thusitha was awarded the outstanding Teaching award in 2010 from the physics department and he has received dissertation completion fellowship 2015 from Missouri S&T as a recognition of outstanding doctoral students.